PEOPLE'S DEMOCRATIC REPUBLIC OF ALGERIA
وزارة التعليم العالي والبحث العلمي
MINISTRY OF HIGHER EDUCATION AND SCIENTIFIC RESEARCH
جامعة عمّار ثليجي بالأغواط
UNIVERSITY AMAR TELIDJI LAGHOUAT
كلية العلوم
FACULTY OF SCIENCES
قسم علوم المادة
Department OF Material Sciences

Master thesis

Domain : Material Sciences
Field : Physics
Option : Material physics

by:
DAGHOR Fella

THEME

On the yet not explored physical properties of the ternary polar intermetalic compounds Na_2CuP and Na_2CuAs: a prediction study by DFT

Publicly defended before the jury consisting of:

Mr. BENMAKHLOUF Abdennour	M.C.A	*President*
Mr. BOUROUROU Yahia	M.C.B	*Examiner*
Mr. HANIFI Mebarki	M.A.A	*Examiner*
Mr. MAABED Said	M.A.A	*Supervisor*

2018/2019

Dedication

Expressions are unable to express the love, esteem, dedication and respect I have for you. Nothing in the world is worth the efforts provided day and night for my education and my vibrancy more than you . my success is the result of your sacrifices you've given me all my life; and each breath i take i am pleased To be your daughter my father DAGHOR Nacer.

My mother DADI ADOUN Aisha, who's worked for my success, by her love, her support, her precious advice. and all the unabated sacrifices that she's made. so for all her assistance and her presence in my life, I want to show her through this modest work my feelings and my eternal gratitude.

To all my siblings: Hocin, Salah Eddin, Hasna and Kaltoum also to all my family DAGHOR and DADDI ADOUN.

My friends around me who have always encouraged me: Sihem, Messaouda, Zoulikha, SELMA, Hana, Feriel, Firouz, Nada....

To the people who always help. stand by me and accompany me on my education trip , to all my colleagues. And all who have contributed as possible to make this project done successfully, I thank you

To all who've sacrificed their time for science. And to all who've benefited the world by science using it for the prosperity of humanity. To all students of the 2018/2019 class.

Fella

Acknowledgment

The synthesis of a dissertation is difficult, however I am delighted to face you my lords,and gratful For allowing me to accomplish this modest work, I want to thank:

the lenient god who enlightened our knowledge path , who gave us the will, the health and the opportunity to fulfill our work perfectly.

I would like to show my deepest thanks to my Mr MAABED SAID assistant professor -A- at the university Ammar Thelidji of Laghouat. I particularly express my gratitude for his patience, encouragement, help, furthermore his dedication to the work during our preparation of this memoir.

Many thank go to Mr BEN MAKHLOUF Abdennour, Mr BOUROUROU Yahia and HANIFI Mebarki for the interest they had to myresearch by agreeing to examine this work and enrich it with their proposals.

I would like to express my sincere thanks to all teachers of physics for their advice and total devotion in teaching us, and a special mention of Mr HELIFA Bachir, Mr HALIT Mohamed, BOUCHENAFA Mohamed, Mr LEFKAIER Ibn Khaldoun, LAGOUNE Brahim, BENTRIA Bachir and...

I am also pleased to my friends, family and every one who have been there for me; especilly my friend HADBI, Roufeida, Louiza, Sami ... I would like to thank them deeply for their support through my journey in the absence of them i would never reach this point..i appreciat that intensely.

TABLE OF CONTENTS

List of abbreviations

BFGS: Broyden-Fletcher-Goldfarb-Shano

DFT: Density Functional Theory

DOS: Density of states

GGA: Generalized Gradient Approximation

GGA-PBE: Generalized Gradient Approximation Perdew-Burk-Ernzerhof.

IBZ: Irreducible Brillouin zone

LDA: Local Density Approximation

PDOS: Partial Density of States

PP: Pseudopotential

PW: Plane Wave

W. P: Wyckoff position

SCF: Self Consistent Field

TB-LMTO: Tight-Binding-Linear Muffin-Tin Orbitals

TDOS: Total Density of States

US-PP: Ultra-soft Pseudopotentials (Ultrasoft pseudopotential)

BZ: Brillouin Zone

List of Figures

Chapter I: Bibliographic review

Chapter II: Theoretical framework

Chapter III: Results and discussion

List of Tables

General Introduction

General Introduction

The rich solid-state chemistry at the border between classical Zintl phases and normal metallic phases provides a fertile area to search for materials with complex crystal structures and intriguing physical properties. Materials belonging to the Zintl border are usually produced by reactions between alkali metals (group 1) or alkaline earth metals (group 2) with transition metals or group elements 13, 14, 15 and 16 of the periodic table of elements. They are very useful in many applications and they include superconducting compounds, thermoelectric materials, hydrogen storage materials, and improved magnetocaloric materials [1].

This work is part of research efforts on the unexplored physical properties of materials at the Zintl border. Particular attention is payed to the ternary alkali metal coper pnictides Na_2CuPn $(Pn = As, P)$ belonging to the family of polar intermetallic phases.

The ternary alkali metal coper pnictides Na_2CuPn $(Pn = As, P)$ are part of a long list of polar intermetallic compounds that have been synthesized by Eisenmann et *al.* [2, 3]. With regard to the abundant literature on the Zintl phases, there is a scarce research material published on these compounds. Indeed, to the best of our knowledge, only their structural properties have been studied [2, 3], thus their physical properties remain out of consideration.

In response to the lack of published research material on the herein considered polar intermetallic phases, this systematic study sought to gather data from reliable first principle methods on their electronic structure, elastic and optical properties. This offers unique opportunity for a wealth of informations to build a knowledge database on their physical properties so far unexplored. The objective is thus threefold: First, to help understand the available experimental data, especially the bonding mechanisms and the mechanical stability of these crystals. Then, to serve as a guide for the experimentation. Finally, to make predictions for new physical properties.

Our day's simulations make it possible to explore the structural, electronic and dynamic properties of matter without prior experimental knowledge of the studied material. In the solid-state physics and in materials science, Density Functional Theory (DFT), developed by Hohenberg-Kohn [4] and Kohn-Sham [5], is currently the most widely used first principle theory. With some practical approximations, DFT based fist principle calculations makes it possible to predict ever more complex materials and new intriguing properties. On the other hand, comparing the results obtained with the available experiments makes it possible to validate the theoretical approaches adopted.

In addition to a general introduction and a general conclusion, this manuscript is structured in three chapters. The first is a bibliographic synthesis on Zintl phases and polar intermetallics. Special attention is paid to the crystalline structure of the considered materials. The second chapter consists of two parts:

- The first part presents an introduction to the fundamentals of density functional theory (DFT), and the approximations used to solve the Kohn-Sham equations. We also present the plane wave approach (PW) for the expansion of Kohn-Sham orbitals, and the pseudopotential approach (PP) as well as the CASTEP code used in this study.
- The second part presents some fundamental knowledge on the elastic properties that we use later in this study.

These first two chapters provide the necessary elements for understanding the subject and locate the work carried out here among all possible investigations. Particular attention is paid the discussion of the results of our calculations in the last chapter. These results were obtained using the methods described in the second chapter.

Finally, in a general conclusion, a summary of the main results obtained in this work is presented.

Bibliographical references

1. Wang, F., *Rationalizing th structures of Zintl and polar intermetallic phases.* 2011.

2. Eisenmann, B., G. Cordier, and H. Schäfer, *CaCuSb (Bi) und SrCuSb (Bi)-Ternäre Phasen im „aufgefüllten "NiAs-(Ni2In)-Typ/CaCuSb (Bi) and SrCuSb (Bi)-Ternary Phases in the „Filled "NiAs-(Ni2In)-Structure.* Zeitschrift für Naturforschung B, 1974. **29**(7-8): p. 457-459.

3. Eisenmann, B., G. Savelsberg, and H. Schäfer, *Zur Darstellung und Kristallstruktur von Na2CuAs, K2CuAs und K2CuSb.* Zeitschrift für Naturforschung B, 1976. **31**(10): p. 1344-1346.

4. Hohenberg, P. and W. Kohn, *Inhomogeneous electron gas.* Physical review, 1964. **136**(3B): p. B864.

5. Kohn, W. and L.J. Sham, *Self-consistent equations including exchange and correlation effects.* Physical review, 1965. **140**(4A): p. A1133.

Bibliographic review

I.1 Introduction

This part is a bibliographic review on the family of Zintl phases A_2BX where A is an alkali metal, B is a transition metal and X is an element of the 15^{th} group of the Periodic Table of Elements. In fact, we first propose a general description of the Zintl phases and polar intermetallic phases. Then we provide a brief history based on works related to the discovery of these materials. We also give a short description of their structural properties. Finally, we will take a look to their technological applications.

I.2 The zintel phases

I.2.1 Définition

Zintl phases are those compounds composed of electropositive metals (e.g. alkali metals, alkaline earth metals, and rare earth metals) and electronegative metals around the "zintl line", which divides columns 13 and 14 in the periodic table. Their name comes from the German chemist Eduard Zintl who was the first to prepare and describe these phases in the $1930s$. The term "Zintl Phase" was first used by F. Laves in 1941. These phases are materials, which contain a block of electropositive elements and a block of electronegative elements. Polar intermetallic phases have the definition similar to Zintl phases but, in general, the electronegativity difference $(\Delta\chi)$ between the constituting electropositive and electronegative metals is smaller than in zintl phases. However, there is no specific critical $\Delta\chi$ that separates Zintl phases and polar intermetallic compounds [1].

Schaefer, Eisenmann and Muller [2] have proposed a more general definition in which the electron transfer for a Zintl phase is essentially complete between the alkaline or alkaline-earth cation and the electronegative elements that attract the electrons by covalent bonding or by formation of isolated lone electrons pairs so that they reach a filled valence band. Therefore, these phases have salt-like characteristics from the ionic bond between the cation and the anionic unit. The later can be isolated anions, and if there are not enough electrons for a full filled shell, they form covalent bonds and poly anionic units[2].

In general, the Zintl phases are compounds which: are brittle with a high melting point, are diamagnetic or exhibit temperature independent paramagnetism, and are narrow-gap semiconductors $(Eg < 1\ eV)$ [2].

On the other hand, rationalizing their structures imposes theoretical challenges because they do not fall into any of the three classical categories of crystalline solids – metallic, ionic, and covalent. This can be conveniently visualized with the van Arkel-Ketelaar triangle (**Figure I.1**). In this triangle, the horizontal axis is the average electronegativity and the vertical axis is the electronegativity difference between the constituting elements. Here the electronegativity values are the so called "absolute electronegativity":

$$\chi = \frac{1}{2}(I + A) \qquad \text{(I.1)}$$

- **I** and **A** are the ionization energy and electron affinity, respectively.

The left base vertex of the triangle represents the classical "metals", where the constituting elements are all electropositive, featuring highly delocalized valence electrons. Starting from the metal vertex, going along the base line, the electronegativity of the constituting elements increases. As a result, valence electrons tend to localize into spaces between atoms and there is the transition from "metallic phases" to "covalent phases". Going from the metal vertex toward the top vertex, the electronegativity difference gets larger and larger. Valence electrons tend to localize around the atoms of the constituting elements with higher electronegativity and there is the transition from "metallic phases" to "ionic phases" [1].

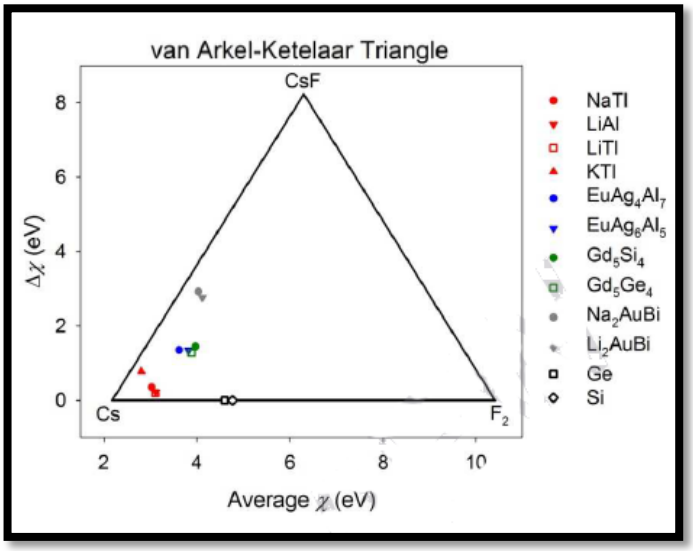

Figure I.1. *The van Arkel-Ketelaar triangle and the locations of the phases investigated [1]*

I.2.2 Zintl Klemm concept

The Zintl–Klemm concept, can effectively rationalize the structures of Zintl phases and polar intermetallic compounds. For example, to rationalize the so-called double diamond structure of $NaTl$, the Zintl–Klemm concept claims that, after obtaining one valence electron from each Na atom, each resulting Tl^- "anion" with four valence electrons will follow the octet rule and form four "covalent" bonds with neighboring Tl^-.

However, the simplicity of the Zintl–Klemm concept also causes its limitations. And so, The electronic structure of $NaTl$ revealed that the Tl 6*s* orbitals are virtually filled, so these electrons are like lone pairs. Therefore, unlike the tetrel atoms in a diamond-type network, the formal "Tl^-" does not involve *sp*3 hybridization. In addition, although most alkali metal trielides adopt the double diamond structure, $LiTl$ adopts the CsCl type structure, and KTl features $[Tl_6]^{-6}$ octahedra. Neither of these two structural exceptions can be understood from this simple formalism. [1].

I.3 Polar intermetallic phases Na_2CuPn (Pn = As, P)

I.3.1 Historical

In 1974, Eisenmann and al. [3] prepared and determined the crystal structure of new ACuX ternary compounds with (A = Ca, Sr and X = Sb, Bi). These compounds are compatible with the structure of NiAs (Ni2In) type. Two years later, they synthesized ternary compounds of general formula A_2BX where A is an alkali metal, B is a transition metal and X is an element of the 15th group of the periodic table. They obtained three polar intermetallic compounds Na_2CuAs, K_2CuAs and K_2CuSb [4]. X-ray diffraction showed that they crystallize in the orthorhombic structure of the Cmcm space group where the two elements B and X form a zigzag chain along the c axis. In 1977, Savelsberg and Schäfer [5] synthesized other new materials with the same structural properties, namely K_2AgX (X = As, Sb and Bi) and Na_2CuP compounds . In 1979, Schuster et al. [6] have prepared a new Na_2AgSb material. The structure of this compound contains Ag-Sb zigzag chains. After a year, Mues and Schuster [7] synthesized three other compounds Na_2AuAs, Na_2AuSb and K_2AuSb. The powder diffraction pattern showed that the Na_2AuAs and Na_2AuSb phases are compatible with the Na_2CuAs structure.

In 2010, Sung-Jin Kim and coworkers. synthesized new polar intermetallic phases of formula A_2AuBi (A = Na, K) and K_2AuSb which also crystallize in the orthorhombic Na_2CuAs type structure [8]. The TB -LMTO calculations show that Na_2AuBi and K_2AuBi are narrow gap semiconductors with 0.5 and ~ 1eV calculated indirect gaps respectively. Analysis of the partial density of states curves showed a covalent interaction between the A and Pn atoms. To our present knowledge, this was one of the few theoretical works devoted to the study of these compounds and there is no other study on their electronic, optical and elastic properties.

I.3.2 Crystallographic structure data for Na_2CuPn (Pn = As, P)

Under normal condition, the polar intermetallic phases Na_2CuPn (Pn = As, P) crystallize in the orthorhombic structure (of space group Cmcm, N °: 63) with four formula units per one unit cell (multiplicity Z = 4).

The conventional cell of this structure contains 16 atoms: 8 atoms of sodium (Na), 4 atoms of copper (Cu) and 4 atoms of arsenic (As) or Phosphorus (P). The arrangement of the atoms is as follows:

- ✓ The Na atoms occupy the 8g site $(x, y, 1/4)$ characterized by the two x and y coordinates that are not fixed by the Cmcm space group.
- ✓ The Cu atoms occupy the 4b site (1/2, 0.0).
- ✓ The As/P atoms occupy the site 4c (0, y, 1/4) also characterized by the coordinate y which is not fixed by the space group Cmcm.

This structure features 2D $[CuPn]_{\infty}^{-2}$ zigzag chains along the c-axis **(Figure I.2)** containing Cu-Pn bonds which acute angle θ at Pn (P, As) **(Figure I.3)** [7] **.** The sodium ions Na^{+}form large channels aligned along the c axis. These channels are occupied by the zigzag chains (**Figure I.4 (b)**). The structural parameters of these two compounds (Na_2CuAs and Na_2CuP) are summarized in **Table I.1.**

Table I. 1: *The mesh parameters and the atomic positions of Na_2AuAs and Na_2AuSb [7].*

lattice parameters (Å)	Na_2CuP			Na_2CuAs		
a	8.67			8.86		
b	6.98			7.22		
c	5.30			5.34		
$\alpha = \beta = \gamma$	90°			90°		
Atomic positions	Na	Cu	P	Na	Cu	As
x	0.3273	0.5	0	0.3262	0	0
y	0.3588	0	0.2405	0.3559	0.5	0.2343
z	0.25	0	0.25	0.25	0	0.25

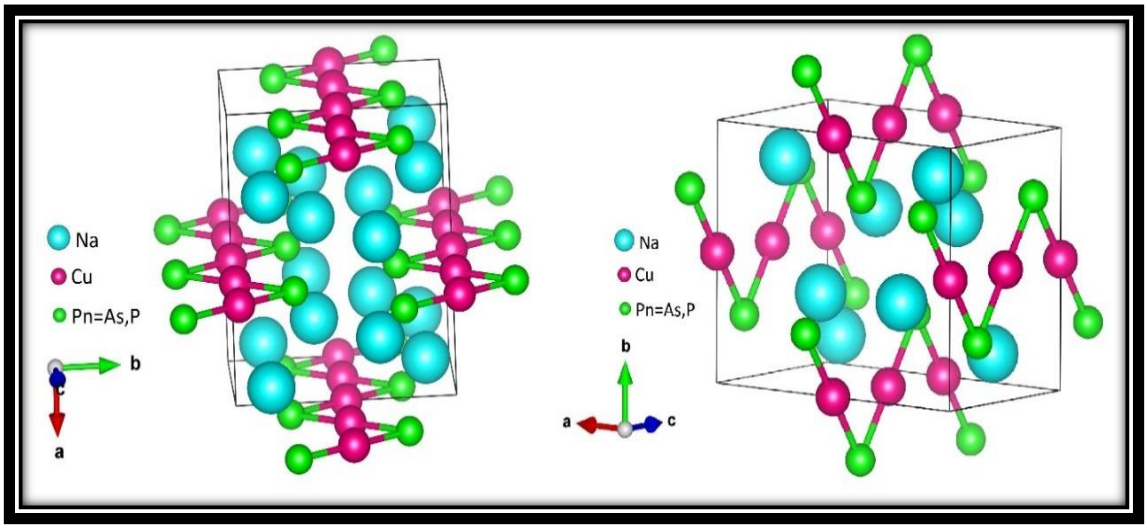

Figure I. 2: *Orthorhombic Structure (Cmcm) of Na_2CuAs and Na_2CuP.*

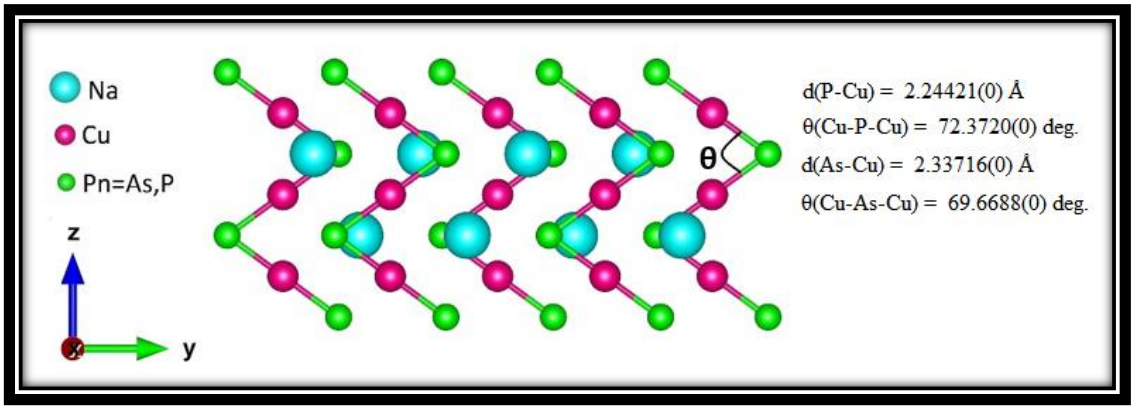

Figure I. 3: *The zigzagg chains Cu-Pn, the interatomic distances (Å), and the angle θ(°) for the compounds Na_2CuPn (Pn = As, P)*

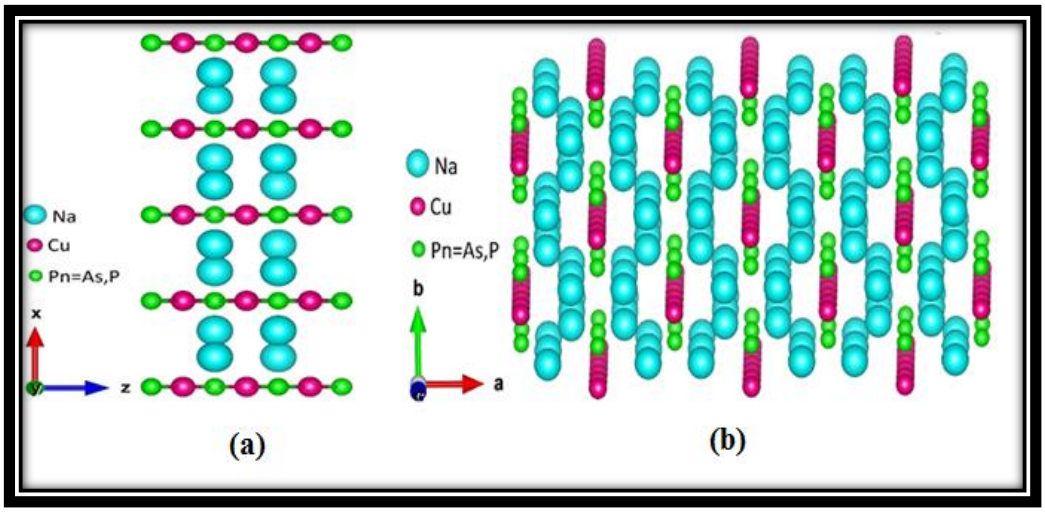

Figure I. 4: *Orthorhombic structure of Na_2CuAs and Na_2CuP: (a) seen along the b axis (b) seen along the c axis .*

Conclusion

To date, polar intermetallic phases remain a rich area to explore. The reasons lie in both their potential technological applications and the theoretical challenges in rationalization of their structures and chemical bonding. Many polar intermetallic phases exhibit new properties. These compounds are therefore promising for many applications, for example: thermoelectric materials, materials for hydrogen storage , and improved magnetocaloric materials [1]. It is therefore important to study their unexplored physical properties to derive new potential applications.

Bibliographical references

1. Wang, F., *Rationalizing th structures of Zintl and polar intermetallic phases.* 2011.
2. Naylor, A., N. White, and I. Nandhakumar, *Electrodeposition of thermoelectric materials.* Thermoelectric Materials and Devices, 2016(17): p. 204.
3. Eisenmann, B., G. Cordier, and H. Schäfer, *CaCuSb (Bi) und SrCuSb (Bi)-Ternäre Phasen im „aufgefüllten "NiAs-(Ni2In)-Typ/CaCuSb (Bi) and SrCuSb (Bi)-Ternary Phases in the „Filled "NiAs-(Ni2In)-Structure.* Zeitschrift für Naturforschung B, 1974. **29**(7-8): p. 457-459.
4. Eisenmann, B., G. Savelsberg, and H. Schäfer, *Zur Darstellung und Kristallstruktur von Na2CuAs, K2CuAs und K2CuSb.* Zeitschrift für Naturforschung B, 1976. **31**(10): p. 1344-1346.
5. Savelsberg, G. and H. Schäfer, *Darstellung und Kristallstruktur von Na2AgAs und KCuS/Preparation and Crystal Structure of Na2AgAs and KCuS.* Zeitschrift für Naturforschung B, 1978. **33**(7): p. 711-713.
6. Schuster, H.-U., C. Mues, and W. Jung, *Darstellung und Kristallstruktur des Na2AgSb/Preparation and Crystal Structure of Na2AgSb.* Zeitschrift für Naturforschung B, 1979. **34**(2): p. 354-355.
7. Mues, C. and H.-U. Schuster, *Na2AuAs, Na2AuSb, K2AuSb-drei neue A2BX-Verbindungen mit BX-Kettenstruktur/Na2AuAs, Na2AuSb, K2AuSb-Three New A2BX Compounds with a BX Chain Structure.* Zeitschrift für Naturforschung B, 1980. **35**(8): p. 1055-1058.
8. Kim, S.J., G.J. Miller, and J.D. Corbett, *Zigzag chains of alternating atoms in A2AuBi (A= Na, K) and K2AuSb. Synthesis, structure, and bonding.* Zeitschrift für anorganische und allgemeine Chemie, 2010. **636**(1): p. 67-73.

Chapter II
The theoretical framework

II.1 Introduction

At the beginning of the 18th century, the laws of classical mechanics did not permit the description of some solid-state phenomena which are related to the behavior of small particles such as electrons**,** nuclei or molecules [1] . In fact, the physical and chemical properties of atomic and molecular systems are governed by the laws of quantum mechanics. These properties have their origin in the behavior of electrons present within such systems and can be evaluated using molecular dynamics calculations, statistical mechanics calculations and quantum mechanical calculation of the electronic structure. The latter uses various mathematical formalisms in order to solve the fundamental equations of quantum mechanics established in this new framework. In this chapter, we will first introduce generalities about the non-relativistic quantum treatment of a system composed of several particles and then, we will discuss the two large families of quantum computations: namely, the Hartree-Fock approximation and the processing of the electronic correlation and the state of the art density functional theory.

II.2 Schrödinger equation

For a solid body consisting of a large number of interacting electrons and nuclei. The equation that describes physical properties (energy, electronics, optics ...) of this quantum system in its fundamental state is the Schrödinger equation, independent of time, written as follows [1].

$$H\Psi(r_i, R_N) = E\Psi(ri, R_N) \tag{II.1}$$

In which

- ✓ Ψ represents the wave function describing the state of the system.
- ✓ $\boldsymbol{r_i}$ the position vector of the electron ***i***.
- ✓ $\boldsymbol{R_N}$ the position vector of the nucleus (ion) **N**.
- ✓ **E** his total energy.
- ✓ **H** represents the total Hamiltonian operator of the system given by the following relation:

$$H = Te(r) + T_N(R) + V_{ee}(r) + V_{NN}(R) + V_{ext}(r, R). \tag{II.2}$$

The Hamiltonian terms of the system are:

- Total kinetic energy of electrons: $\mathrm{T_e(r)} = \frac{-\hbar^2}{2\mathrm{m}} \sum_{\mathrm{i}} \Delta_i$ (II.3)
- Total kinetic energy of the nuclei: $\mathrm{T}_N\mathrm{(R)} = \frac{-\hbar^2}{2\mathrm{M}} \sum_{\mathrm{k}} \Delta_k$ (II.4)

- Interaction energy between electrons: $V_{ee}(r) = \frac{1}{2}\sum_{i,j\neq i}\frac{e^2}{4\pi\varepsilon_0|\vec{r_i}-\vec{r_j}|}$ (II.5)
- Potential energy between electrons and nuclei: $V_{ext}(r,R) = -\sum_{i,k}\frac{Z_k e^2}{4\pi\varepsilon_0|\vec{R_k}-\vec{r_i}|}$ (II.6)
- Potential energy between nuclei: $V_{NN}(R) = \frac{1}{2}\sum_{k,l\neq k}\frac{e^2 Z_k Z_l}{4\pi\varepsilon_0|\vec{R_k}-\vec{R_l}|}$ (II.7)

- ✓ $\boldsymbol{M}$ the mass of the nucleus $\boldsymbol{K}$.
- ✓ $\boldsymbol{m}$ the mass of the electron $\boldsymbol{i}$ and $\boldsymbol{e}$ its charge.
- ✓ $\boldsymbol{ri, j}$ and $\boldsymbol{RK, l}$: electronic coordinates (i and j) and nuclei (k and l) respectively.
- ✓ $\boldsymbol{Zk, l}$: the atomic number of the nuclei k and l.
- ✓ $(\boldsymbol{R_k} - \boldsymbol{R_l})$, $(\boldsymbol{r_i} - \boldsymbol{r_j})$ and $(\boldsymbol{R_k} - \boldsymbol{r_l})$ are respectively interatomic distances, interelectronic and between the electron and the nucleus.

In order to simplify the writing of the equations, we use the atomic units (Ua) the following table summarizes these units:

Table II.1: *Atomic unit used in DFT and their equivalents in the international system (SI)*

Quantité	Symbole	Unite (SI)	Unité atomique(**u. a**)
Masse	m_e	9.1096×10^{-31}kg	**1u.a**
Charge	E	-1.6022×10^{-19}C	**1u.a**
Longueur	(le rayon de Bohr)a_0	0.52918×10^{-31}m	**1u.a=1(Bohr)**
Energie	E (Hartree)	4.359743×10^{-18} J	**1u.a=1(Hartree)**
Action	$\hbar = h/2\pi$	1.0646×10^{-34}J.s	**1u.a**

The Schrödinger equation is written as follows:

$$H\psi = \frac{-\hbar^2}{2M}\sum_k \Delta_k + \frac{-\hbar^2}{2m}\sum_i \Delta_i + \frac{1}{2}\sum_{i,j\neq i}\frac{e^2}{4\pi\varepsilon_0|\vec{r_i}-\vec{r_j}|} + -\sum_{i,k}\frac{Z_k e^2}{4\pi\varepsilon_0|\vec{R_k}-\vec{r_i}|} + \frac{1}{2}\sum_{k,l\neq k}\frac{e^2 Z_k Z_l}{4\pi\varepsilon_0|\vec{R_k}-\vec{R_l}|} \quad \text{(II.8)}$$

All the observable properties of the electron-nucleus system are contained in this equation. It is therefore sufficient to solve it in order to have access to the states of the system and its physical properties. However, it is not possible to solve rigorously such equation, since it is a correlated wave function between all the particles, the complexity of this equation grows exponentially with the number of particles. Therefore, approximations had to be introduced in order to solve this equation. We begin with the first approximation introduced by Born-Oppenheimer.

II.3 The Born-Oppenheimer Approximation

The first approximation made to solve equation **(II.1)** is the adiabatic approximation [2] made in 1926 by Born and Oppenheimer. It is based on the very large difference between the masses of nuclei and electrons (it is less than 10^{-5} for atoms heavier than calcium). As a result, the electronic relaxation is instantaneous with respect to the movement of the nuclei. Then one can write the system's wave function as a product of two wave functions; one for the nuclei and the other for the electrons which is the electronic wave function. Thus, the potential energy V_{NN} becomes a constant. Thus, the electronic part of the Hamiltonian of the system equation **(II.8)** becomes:

$$H_e = T_e + V_{ee} + V_{Ne} \quad \text{(II.9)}$$

The solution of the Schrödinger equation with this Hamiltonian is given by:

$$H_e\psi = E_e\psi \quad \text{(II.10)}$$

Although this approximation greatly simplifies equation **(II.1)** by uncoupling electron movement of that of the nuclei, the equation **(II.10)** still cannot be solved exactly because of the poly-electronic nature of the system's wave function due to the interacting electrons. Therefore, it is necessary to apply other simplifications.

II.4 Hartree and Hartree-Fock approximation

Hartree proposed a second approximation in 1928. The idea is to assume that the electrons move independently of each other. That is to say that the probability of finding the coordinate electron $\boldsymbol{r1}$ in the orbital 1 is independent of that of other electrons.

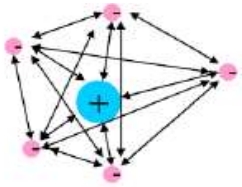

Figure II.1: *Many-electron systems. All electron- electron repulsion is included explicitly*

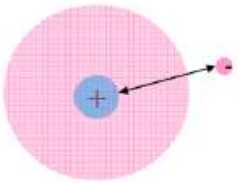

Figure II.2: *one-electron systems with remaining electrons represented by an average charge density*

Then the electronic wave function can be written as a product of electronic mono waves [3]:

$$\Psi_e\,(r1, r2, \ldots\ldots rn) = \Psi_1(r_1).\Psi_2(r_2).\Psi_3(r_3)\ldots\ldots\Psi_n(r_n) \quad \text{(II.11)}$$

The Schrödinger equation to a particle called Hartree's equation is written in the form:

$$\left[-\frac{\hbar^2}{2m}\Delta_i + U_i(r_i) + V_i(r_i)\right]\Psi_i(r) = \varepsilon_i\Psi_i(r) \quad \text{(II.12)}$$

The general algorithm followed to solve these equations is said self-coherent or SCF (self consists Field).

However, this approximation which is based on the assumption of independent electrons and which neglects the interaction of electrons with spin states, does not prevent two electrons to occupy the same quantum state. This violates Pauli's exclusionary principle that wave function of the fermions system must be antisymmetric with respect to the exchange of two particles.

To correct all that, Hartree and Fock proposed to express the multi electronic wave function in the form of a Slater determinant:

$$\Psi_e = \Psi(r_1, r_2, r_3, \dots, r_n) = \frac{1}{\sqrt{N!}}\begin{bmatrix}\Psi_1(r_1) & \Psi_1(r_2) \dots \dots \dots & \Psi_1(r_n)\\ \Psi_2(r_1) & \Psi_2(r_3) \dots \dots \dots & \Psi_2(r_n)\\ \Psi_3(r_1) & \varphi_3(r_2) \dots \dots \dots & \Psi_3(r_n)\\ & . & \\ & . & \\ & . & \\ \Psi_n(r_1) & \Psi_n(r_2) \dots \dots \dots & \Psi_n(r_n)\end{bmatrix} \quad \text{(II.13)}$$

Where each wave function $\Psi_i(r_i)$ is called spin orbital, because it is composed of two parts: an orbital function and the other is a spin function (up or down), and $\frac{1}{\sqrt{N!}}$ is here normalization constant.

This new multi electronic wave function is anti-symmetric with respect to the exchange of two particles; hence, Pauli's principle is respected. The Slater's determinant is calculated using the variational principle.

The application of the Hamiltonian on the wave function gives the Hartree-Fock energy:

$$E_{HF}\,\Psi_i(r_i) = \left(-\frac{\hbar^2}{2m}\nabla^2 r_i + V_{eN}\,(r_i) + \sum J_J\, - K_J\right)\Psi_i\,(r_i) \quad \text{(II.14)}$$

The operator in parentheses is the Fock operator in which the term $-\frac{\hbar^2}{2m}\nabla^2 r_i$ corresponds to the kinetic energy of the electron i. The operator $V_{eN}\,(r_i)$ describes the electrostatic interaction between this electron and the nucleus (s). The operator j_j is called Coulombian operator, and it represents the average potential created by the other electrons, while k_j is the exchange operator which represents the correction to this potential due to antisymmetry.

The function given by equation **(II.14)** leads to the Hartree-Fock equations for a one-particle system:

$$\left[-\frac{1}{2}\nabla_i^2 + V_{ext}(\vec{r},\vec{R}) + \sum_{\substack{j=1 \\ j\neq 1}}^{n} \int \frac{|\Psi_j|\overrightarrow{r'}|^2}{|\vec{r}-\overrightarrow{r'}|}\overrightarrow{dr'}\right]\Psi_i(\vec{r}) - \sum_{\substack{j=1 \\ j\neq 1}}^{n} \int \frac{\Psi_j(\vec{r})\Psi_j^*(\overrightarrow{r'})}{|\vec{r}-\overrightarrow{r'}|}\overrightarrow{dr'}\,\Psi_i(\overrightarrow{r'}) = \varepsilon_i\Psi_i(\vec{r_i}) \qquad (\text{II.15})$$

Whereas Hartree's method does not take into account the far-fetched fact of two electrons of the same spin in the same quantum state, the Hartree-fock method makes it possible to fill this gap by introducing these quantum effects designated by the exchange term (last term of equation **(II.15)**). The difference between the energy of the ground state of the system determined from equation **(II.12)** and that determined from equation **(I.15)** is the exchange energy.

Let us recall that electron-electron interactions are described in this model as the interactions of each electron with a mean field due to other electrons, which means to neglect the electronic correlation. The difference between the energy of the true ground state and that determined from equation **(I.15)** is the correlation energy.

The Hartree-fock approach works well when it comes to dealing with small systems ie molecules, so it is often used by chemists to determine the ground state energy of small molecules. However, it doesn't give a good description for large systems, because it neglects the electronic correlations [4]. It is therefore necessary to carry on with another theoretical framework that overcomes this limitations.

II.5 Density functional theory (DFT)

The fundamental concept of this theory is that the energy of an electronic system can be expressed as a function of its density. It is in fact an old idea that goes back mainly to the works of Thomas [5] and Fermi [6] who tried to express the total energy of a system according to its electronic density by representing its kinetic energy according to a functional of this magnitude.

II.5.1 Thomas –Fermi model

The **Thomas–Fermi** (**TF**) **model** [5, 6] named after Llewellyn Thomas and Enrico Fermi, is a quantum mechanical theory for the electronic structure of many-body systems developed semiclassically shortly after the introduction of the Schrödinger equation. [7] It stands separate from wave function theory as being formulated in terms of the electronic density alone and as such is viewed as a precursor to modern density functional theory. The TF model is correct only in the limit of an infinite nuclear charge. Using the approximation for realistic systems yields poor quantitative predictions, even failing to reproduce some general features of the density such as

shell structure in atoms and Friedel oscillations in solids. It has however found modern applications in many fields through the ability to extract qualitative trends analytically and with the ease at which the model can be solved. The kinetic energy expression of Thomas–Fermi theory is also used as a component in more sophisticated density approximation to the kinetic energy within modern orbital-free density functional theory.

Working independently, Thomas and Fermi used a statistical model in 1927 to approximate the distribution of electrons in an atom. Although electrons are distributed no uniformly in an atom, an approximation was made that the electrons are distributed uniformly in each small volume element ΔV (i.e. locally) but the electron density $n(\overrightarrow{r})$ can still vary from one small volume element to the next.

$$E_0 = [n] \qquad (\text{II.16})$$

$$T_{TF} = [n] = \int t\left[n(\overrightarrow{r})\right] dr \qquad (\text{II.17})$$

$$t\left[n(\overrightarrow{r})\right] = \frac{3}{5}\, n(\overrightarrow{r}) E_F \qquad (\text{II.18})$$

$$E\left[\overrightarrow{\Psi}\right] = E[n] = T[n] + U_{ee}[n] + \int U_{ext}(\vec{r}) n(\overrightarrow{r}) dr \qquad (\text{II.19})$$

$t\left[n(\overrightarrow{r})\right]$: represent the kinetic energy density of electrons system without interaction.

If the electronic density of a system whatever is given, this functional allows to calculate explicitly the total energy, which we obtain the minimization of the functional over all possible densities.

Both authors have neglected the effects of exchange and correlation that arise between electrons. However, this defect was corrected by Dirac [8], who introduced the exchange approximation of the electron density.

The idea of Hohenberg and Kohn in 1964 [9] was later to generalize this approach to any electronic system by two theorems.

II.5.2 Hohenberg-Kohn theorems

The basic formalism of the DFT is based on the Hohenberg-Kohn theorem (1964) [9].

This approach is based on two theorems:

- **Theorem 1:**

The electronic density ρ (r) is the only function necessary to obtain all the properties of any system. In other words, there is a one-to-one correspondence between the electronic density of the

ground state $\rho_0\ (r)$ and the external potential $V_{ext}\ (r)$ and therefore between $\rho_{fond}\ (r)$ and the ground state wave functionΨ_{fond}.

$$E = E[(\rho_{fond})] = F_{HK}[(\rho_{fond})] + \int V_{en}(r)\rho(r)dr \quad \text{(II.20)}$$

With:

$$F_{HK}[(\rho_{fond})] = T[\rho(r)] + V[\rho(r)]. \quad \text{(II.21)}$$

Or:

- ✓ $\boldsymbol{T}\ [\boldsymbol{\rho}\ (\boldsymbol{r})]$: is the kinetic energy of the electronic system.
- ✓ $\boldsymbol{V}\ [\boldsymbol{\rho}\ (\boldsymbol{r})]$: is the term of electron-electron interactions.
- ✓ $\boldsymbol{F_{HK}}[(\boldsymbol{\rho_{fond}})]$: The functional of Hohenberg and Kohn.

The first theorem does not give us sufficient information that determines whether any density is that of the ground state. This is the object of the second theorem of Hohenberg and Kohn.

Theorem 2:

This theorem shows that the energy functional $E\ [\rho]$ is minimum when any electronic density $\rho\ [r]$ corresponds to the electronic density of the ground state $\rho_{fond}(r)$

$$E[(\rho_{fond})] = MinE\rho \quad \text{(II.22)}$$

That is, according to the first theorem, a test electron density ρ_{test} defines its own Hamiltonian and likewise its own test wave function Ψ_{test} . From there, we can have a correspondence between the variational principle in its wave function version and in its electronic density version such that:

$$\langle \Psi\text{test}|H|\Psi\text{test}\rangle = E[\rho test] \geq Efond = \langle \Psi\text{fond}|H|\Psi\text{fond}\rangle \quad \text{(II.23)}$$

In summary: all the properties of a system defined by an external potential V_{ext} can be determined from the electronic density of the ground state. The energy of the system $E(r)$ reaches its minimum value if and only if the electronic density is that of the ground state.

However, there remains a major problem to be solved, how to rewrite an exact analytical formulation of the functional $F_{HK}[\rho]$ for an interacting N electron system.

- ✓ $\boldsymbol{V_{H(r)}}$: the electronic potential of Hartree which is expressed by:

$$V_H(r) = \frac{e^2}{2}\int \frac{n(r)n(r')}{|r-r'|} d^3r d^3r' \quad \text{(II.24)}$$

- ✓ $\boldsymbol{V_{xc}[n(r)]}$:the potential of exchange and correlation obtained by the simple derivative of the exchange energy and correlation with respect to the electronic density:

$$Vxc(r)=\frac{\partial Exc[n(r)]}{\partial n(r)} \quad \text{(II.25)}$$

As each electron goes through the effect of the effective potential created by all other electrons, the equations of Kohn and Sham become:

$$H\Psi_i = [\frac{\hbar^2}{2m}\nabla^2 + V_{eff}\,(r)]\Psi_i(r) = E_i\Psi_i \quad \text{(II.26)}$$

II.5.3 Kohn-Sham equations

Kohn and Sham have introduced the idea in which the interacting multi-particle physical system is replaced by a fictitious system of independent particles, which is easier to solve. Kohn and sham have assumed that the electron density of the ground state of the real system is equal to that of the fictitious system

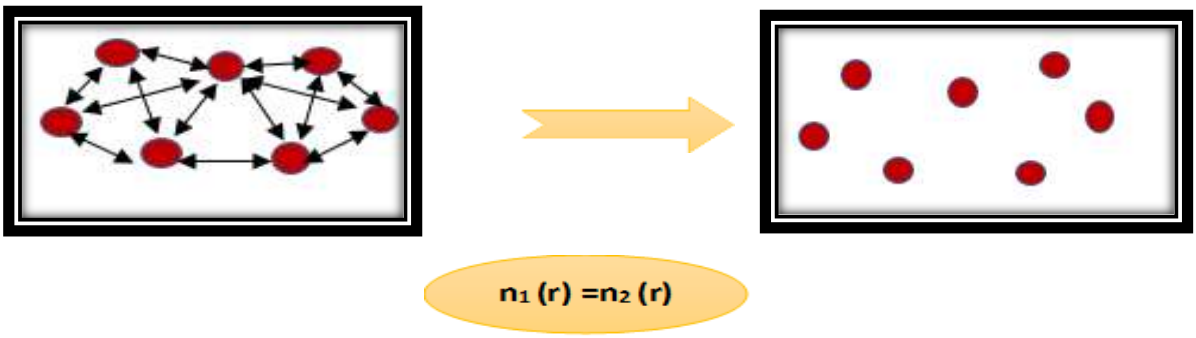

Figure II.3 *the real system and the effective system with the same density.*

This leads to solving a set of equations for independent particles like those of Hartree or Hartree-fock:

$$H_{KS}\Psi_i(\vec{r}) = \varepsilon_i\Psi_i(\vec{r}) \quad \text{(II.27)}$$

With:

$$H_{KS} = -\frac{1}{2}\nabla_i^2 + U_{eff}(\vec{r}) \quad \text{(II.28)}$$

And:

$$U_{eff} = U_{ext}(\vec{r}) + \underbrace{\int \frac{n(\vec{r'})}{|\vec{r}-\vec{r'}|}\,dr'}_{U_H(\vec{r})} + U_{xc}(\vec{r}) \quad \text{(II.29)}$$

Where:

- ✓ $U_{ext}(\vec{r})$ is extern potential.
- ✓ $U_H(\vec{r})$ is Hartree potential.
- ✓ $U_{xc}(\vec{r})$ is exchange potential.

The problem is that the exchange and correlation energy cannot be handled accurately; therefore, we must make approximations.

II.5.4 The exchange and correlation functional

II.5.4.1 Local density approximation (LDA)

Assumes that the electron density at a point r depends only on the density in r, and that it is equal to the correlation energy per particle of a homogeneous gas of density n(r):

$$E_{xc}^{LDA}[n(\vec{r})] = \int n(\vec{r})\varepsilon_{xc}^{LDA}\big(n(\vec{r})\big)\,dr \qquad \text{(II.30)}$$

Or the exchange-correlation energy can be decomposed as the sum of the exchange energy and the correlation energy.

$$\varepsilon_{xc}^{LDA}[n(\vec{r})] = \varepsilon_x[n(\vec{r})] + \varepsilon_c[n(\vec{r})] \qquad \text{(II.31)}$$

The term exchange energy is known, it is given by functional energy exchange of Thomas-Fermi-Dirac:

$$\varepsilon_x^{LDA}(\vec{r}) = -\frac{3}{4}\left(\frac{3}{\pi}\right)^{\frac{1}{3}} n(\vec{r})^{\frac{1}{3}} \qquad \text{(II.32)}$$

On the other hand, the correlation energy, which is more complex to evaluate, is assessed via quantum Monte Carlo-methods **[10]**.

II.5.4.2 Generalized Gradient Approximation (GGA)

The LDA approach is based on the homogeneous electrons gas model, and therefore assumes a uniform electron density. However, atomic or molecular systems are most often very different from a homogeneous electron gas, in a more general way, we can consider that all real systems are inhomogeneous, which means the electronic density has a spatial variation (locale) **[11]**.

Most of the corrections that have been introduced at the LDA are based on the idea of taking into account local variations in density. For this reason, the gradient of the electronic density has been introduced leading to the approximation of the generalized gradient (GGA), in which the exchange-correlation energy and is depending on the electron density and its gradient:

$$E_{xc}^{GGA}[n(\vec{r}), \nabla n(\vec{r})] = \int n(\vec{r})\varepsilon_{xc}^{GGA}\,[n(\vec{r}), \nabla n(\vec{r})]dr \qquad \text{(II.33)}$$

There are many expressions to describe the GGA functional following the choice of $\varepsilon_{xc}[n(\vec{r}), \nabla n(\vec{r})]$ as forms of Becke (B88) [12]. from Perdew-Wang (PW91)[13] and Perdew-Burke- Ernzerhof (PBE)[14] Hansen and Norskov (RPBE)[15] .

II.5.4.3 Hybrid Functional

In DFT calculations, the use of LDA or GGA allows an accurate description of energy related physical properties such as equilibrium geometry and elastic properties. However, the use of these two approximations still generates some significant errors especially when calculating the ground state energy of small molecules and the semiconducting band gaps for extended systems.

In order to compensate for these flaws, a new generation of exchange-correlation functionals has been recently developed. In these models, the exchange-correlation energy functional mixes both Hartree-Fock and other formalism of the DFT (LDA or GGA). Currently, the most common hybrid functional are PBE0, HSE03, HSE06 and B3LYP [16]. The use of such functionals makes it possible reproduce accurately the experimental data.

In general, hybrid functionals are particularly effective for the description of molecules , insulators, semiconductors and transition metal oxides. Their major disadvantage is that such calculations are computationally more expensive than the conventional functional, because of the incorporation of Hartree-Fock terms.

II.6 Solving the equations of kohn-sham

To solve the Kohn-Sham equations, one must choose a basis set for the wave functions that can be taken as a linear combination of orbitals, called Kohn-Sham orbitals (KS) written in the form:

$$\Psi_i(\vec{r}) = \sum C_{ij} \emptyset_j(\vec{r}) \qquad \text{(II.34)}$$

Where $\Phi_J(\vec{r})$ are the basis functions and C_{IJ} the development coefficients.

The resolution of the Kohn and Sham equations comes down to the determination of the coefficients C_{IJ} for occupied orbitals which minimize the total energy. The resolution of the KS equations for symmetry points in the first Brillouin zone simplifies the calculations. This resolution is done in an iterative manner using an auto coherent iteration cycle as illustrated by the flowchart of Figure (II.1). We start by injecting the initial charge density $\rho_{in}$to diagonalize the secular equation:

$$(H_{\varepsilon i} S) C_i = 0 \qquad \text{(II.35)}$$

Where *H* represents the Hamiltonian matrix and *S* the overlay matrix. Next, the new charge density ρ_{out} is constructed with the eigenvectors of this secular equation using the total charge density that can be obtained by summation over all occupied orbitals.

If the calculations do not match, the two densities ρ_{in} and ρ_{out} are mixed in the following way:

$$\rho_{in}^{i+1} = (1-a)\rho_{in}^{i} + a\rho_{out}^{i} \quad \text{(II.36)}$$

i represents the i th iteration and α is a mixing parameter. Thus, the iterative procedure can be continued until convergence is achieved.

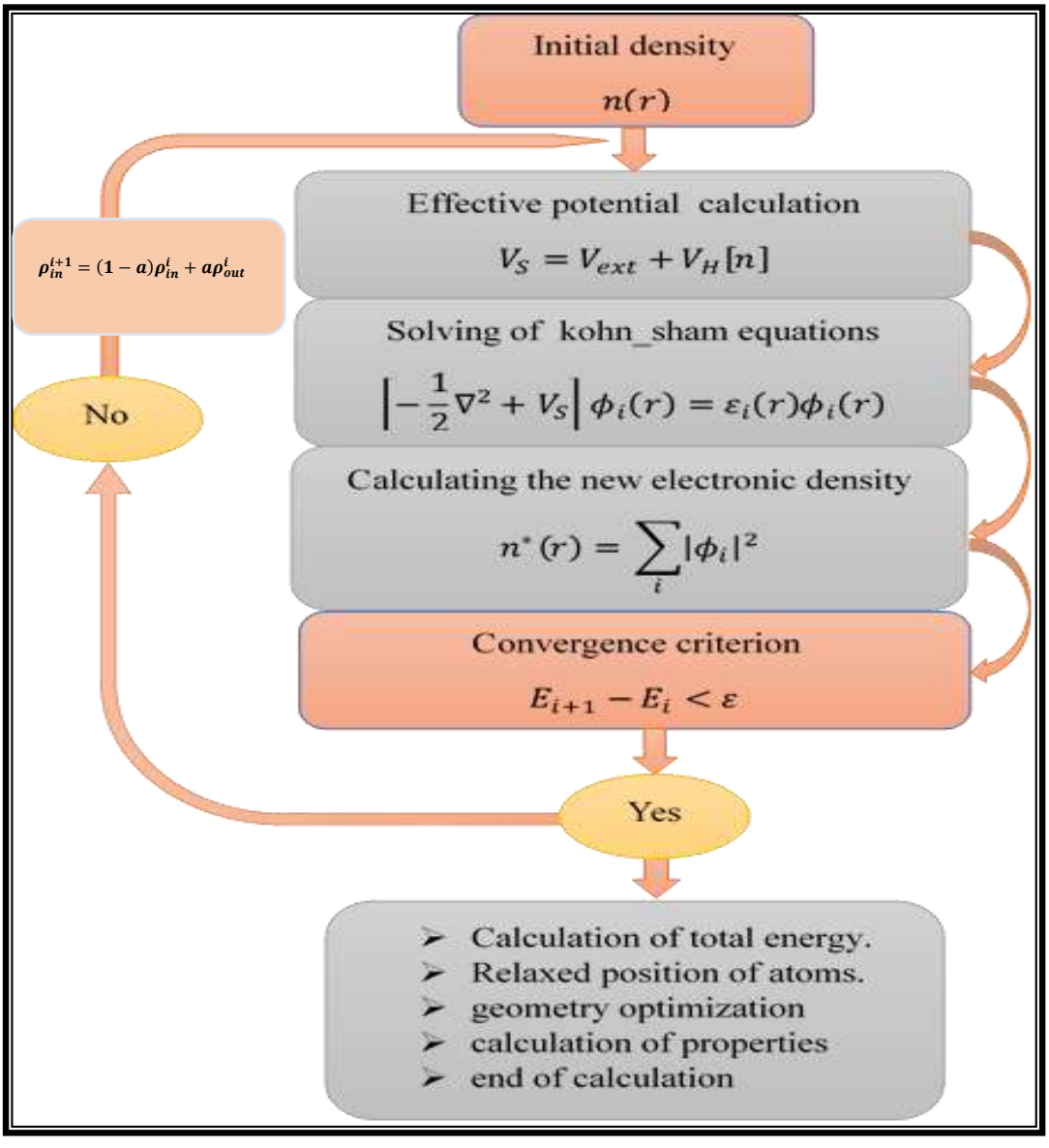

Figure II.4: *Diagram describing the iterative process for solving the Kohn-Sham equations [17]*

II.7 Practical implementations of the DFT

To solve the DFT equations (Kohn and Sham equations), numerical processing introduces additional approximations, which are nevertheless controlled by the user of an ab-initio calculation code. In this section, we will give an overview of the main numerical approximations: the sampling of the zone of Brillouin or grid of K points, and cutoff energy which defines the size of the plane wave base used in the serial development of Bloch functions.

II.7.1 Periodic Systems and Bloch theorem

Bloch theorem is a consequence of the periodicity of the crystalline potential [18];it illustrates the invariance of the system by translational symmetry. The wave function is then written as the product of a periodic function, U_J^K owning the periodicity of the lattice, and a plane wave.

$$\Psi_J^K(\vec{r}) = U_J^K(\vec{r})e^{i(\vec{k},\vec{r})} \quad \text{(II.37)}$$

$$U_J^K(\vec{r}) = \sum_G \breve{U}(\vec{G})e^{i(\vec{G},\vec{r})} \quad \text{(II.38)}$$

The vectors $\vec{K}$ and $\vec{G}$ are defined in reciprocal space within the first zone Brillouin. Solving Kohn and Sham equations within a periodic system is done necessarily for a finite number of points K points obtained by an appropriate representative sampling of the ZB that allows to reproduce faithfully its symmetry.

II.7.2 Sampling of the Brillouin Zone (BZ)

Brillouin-zone sampling in total-energy calculations of aperiodic systems using periodic boundary conditions is considered. Although the energies converge to the exact result in the limit of large supercells for any k-point sampling scheme, they do not converge at the same rate. In particular, shown that the use of a single sampling point at the origin of reciprocal space is especially inefficient. An appropriate and representative k-point sampling scheme is proposed by Monkhorst and Pack method, which is computationally efficient [19].

II.7.3 The plane wave base: the cutoff energy

In order to develop a real calculation, it is necessary to choose a base of functions to express the wave functions. Therefore, it is better to use a plane wave basis set.

The plane wave decomposition of wave functions $\varphi_J^K(\vec{r})$ consists in expressing these wave functions using Fourier series:

$$\varphi_J^K(\vec{r}) = \Omega^{-1/2} \sum_G C_J^K e^{i(\vec{k}+\vec{G})\vec{r}} \quad \text{(II.39)}$$

Theoretically, to describe a monoelectronic wave function, it would logically be an infinite number of plane waves. Nevertheless, in practice, this number is limited by a cut-off energy (E_{cut}), which represents a stopping criterion corresponding to a minimization of the error made at the level of the kinetic energy (the plane waves being functions proper of the operator kinetic energy):

$$\frac{1}{2}\left|\vec{k}+\vec{G}\right|^2 < E_{cut} \qquad \text{(II.40)}$$

The truncation of the base will bring errors on the calculation of the total energy. These errors can be manipulated by increasing the cutoff energy, so the base is extended (Increase in the number of plane waves) and thus improve the accuracy of calculations, but as a result the calculation time increases sharply. So, we have to find a compromise between the cut-off energy and the computation time, for which the total energy converges with the required precision, so that it is necessary to carry out convergence studies before interpreting the results. The value of the cut-off energy E_{cut} depends on the considered system and in particular on the choice of the pseudo-potential.

II.7.4 Pseudopotential method

The pseudopotential method is based on the assumption that only valence electrons (the outermost electrons) contribute significantly to the physical and chemical properties of a given electronic system. The valence electrons are the only ones involved in the chemical bonding picture, whereas the core electrons (the most internal electrons) are not strongly sensitive to the chemical environment. Ionic cores (nuclei and core electrons) are thus considered to be "frozen" in their atomic configurations; it is the approximation of the frozen heart **[20].** So, this method is to deal explicitly only with the valence electrons, which then move in an effective potential, produced by these inert ionic cores, called **pseudopotential.**

The wave functions of the valence electrons oscillate rapidly in the region near the nucleus. They therefore remain difficult to describe from a high plane wave base. The part of the near-ionic wave function is then replaced by fictitious wave functions, or pseudo-wave functions, which give rise to the same valence wave functions beyond a certain cut-off radius r_c. These wave pseudo-wave functions are then "softer" than the real wave functions. It is also said that the very "hard" potential of the ionic core is replaced by a «softer» pseudopotential, for:

$$|r| > r_c\,, V_{ps}(r) = V(r)\ et\ \varphi^{ps}(r) = \varphi^{AE}(r)$$

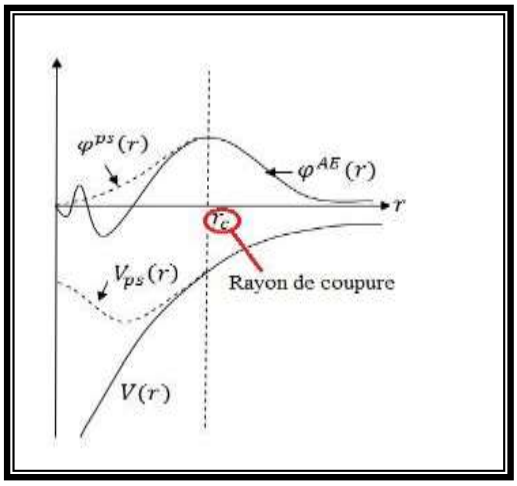

***Figure II.5**: Comparison of a wave function in the coulomb potential of the nucleus to the one in the pseudopotential. The real and the pseudo-wave function and potential match above a certain cutoff radius [21].*

The use of the pseudopotential approach makes it possible to reduce the number of electrons to be taken into account in the calculations (since it deals explicitly only with the valence electrons), therefore the number of plane waves necessary for the description of the wave functions is greatly reduced. This leads to reducing the calculation volume, then a saving of execution time. The methods of pseudopotential construction are divided into categories according to the basis used to develop the pseudo-functions, we cite as an example: the norm conserving pseudopotentials (NC-PP) and the ultrasoft pseudopotentials (US-PP). In this study Vanderbilt pseudo-potentials [22], also called "ultrasoft" pseudopotentials were used. These pseudopotentials are characterized by arbitrarily soft wave pseudo-functions in the heart regions.

II.8 Calculation Code: CASTEP

All the calculations presented in this manuscript were performed using the CASTEP code (Cambridge Serial Total Energy Package) [23].This code was originally developed in 1988 by Payne et al [24]. CASTEP is a DFT and a molecular dymanics (MD) based calculation code. It is part of a set of digital simulation software named Materials Studio (MS) and commercialized by Biovia from Dassault Systems.

CASTEP is developed by Condensed Matter Theory Group at the University of Cambridge, UK, it's a program that uses the density functional theory (DFT) to simulate the properties of materials. It can predict many key properties, including elastic constants, equilibrium geometry, energy band diagrams, total and orbital projected partial electronic densities of state, charge densities, optical properties as well as vibrational and thermodynamic properties. This code is used to simulate the total energy by special integration of K-points in the first Brillouin zone with a plane wave base expansion of wave functions and the summation is performed on the wave vectors

produced by the Monkhorst and Pack method [25]. CASTEP runs on Windows and Linux. A graphical user interface that complies with Microsoft Windows standards, allows the user to interact with the 3D graphical representation of structures and molecules, configure calculations and analyze results through simple dialogs and a familiar Windows environment.

II.9 Elastic properties of the solid

The elastic properties of solids are closely related to several fundamental properties of the solid state, such as specific heat, thermal expansion, Debye temperature. The analysis of the elastic behavior of a material is reduced to the determination of the corresponding elastic constants; these constants provide information on the nature of the chemical bonds in the solid, its rigidity, its elastic anisotropy and its mechanical stability.

II.9.1 Elasticity of isotropic solids

A medium is said to be elastic if it undergoes only reversible deformations, by removing the forces responsible for these deformations, the medium returns to its original shape. In the field of elasticity, the deformation is linearly proportional to the stress applied according to Hooke's law, this law is valid in the limit of small deformations for isotropic materials (in an isotropic material, all directions are identical). The stress can be represented as a tensorσ_{ij} such that the index i indicates the direction of the force, and the index j refers the normal to the plane on which the force applies.

In linear elasticity theory, there is a linear relation between $\sigma$and ε given by the generalized Hooke law:

$$\sigma_{ij} = C_{ijkl}\varepsilon_{kl} \tag{II.41}$$

Where $i, j, k, l = 1,2,3$ and C_{ijkl} is a tensor of order 4 called tensor of elastic rigidity and it defines the elastic constants of the material. One can define reciprocally the tensor of the constants of deformability (tensor of the supplications) S_{ijkl} by the following relation:

$$\varepsilon_{ij} = S_{ijkl}\sigma_{kl} \tag{II.42}$$

Due to the symmetry of the stress tensor $(\sigma_{ij} = \sigma_{ji})$and the deformation tensor, $(\varepsilon_{ij} = \varepsilon_{ji})$ the number of independent components of C_{ijkl} is reduced to 36 (6 × 6 matrix). In contracted notation of Voigt (transformation of the indices), the matrix expression of the rigidity components is simplified, C_{ijkl} becomes C_{ij} $(i, j = 1\ to\ 6)$. Similarly, for the deformability constants.

Thus, Hooke's law is put in the following matrix form:

$$\underbrace{\begin{bmatrix}\sigma_{11}\\ \sigma_{12}\\ \sigma_{13}\\ \sigma_{14}\\ \sigma_{15}\\ \sigma_{16}\end{bmatrix}}_{\text{Constraints}} = \underbrace{\begin{bmatrix}C_{11} & C_{12} & C_{13} & C_{14} & C_{15} & C_{16}\\ C_{21} & C_{22} & C_{23} & C_{24} & C_{25} & C_{26}\\ C_{31} & C_{32} & C_{33} & C_{34} & C_{35} & C_{36}\\ C_{41} & C_{42} & C_{43} & C_{44} & C_{45} & C_{46}\\ C_{51} & C_{52} & C_{53} & C_{54} & C_{55} & C_{56}\\ C_{61} & C_{62} & C_{63} & C_{64} & C_{65} & C_{66}\end{bmatrix}}_{\text{Constants of elasticity}} \underbrace{\begin{bmatrix}\varepsilon_{11}\\ \varepsilon_{12}\\ \varepsilon_{13}\\ \varepsilon_{14}\\ \varepsilon_{15}\\ \varepsilon_{16}\end{bmatrix}}_{\text{Deformation}} \qquad \text{(II.43)}$$

The inverse of the stiffness matrix is the flexibility matrix$S_{ij} = (C_{ij})^{-1}$, which contains the same number of constants. The number of independent elastic constants C_{ij} required to describe the elastic behavior of a crystalline solid depends on its symmetry. It increases if the symmetry is reduced, if the crystal has a triclinic symmetry, for example, the total number of C_{ij} is equal to 21. **Table II.1** shows the number of independent elastic constants for each crystalline system.

***Table II.2**: The number of elastic constants C_{ij} for each crystalline system.*

Crystalline systems	Number of C_{ij}
Triclinique	21
Monoclinique	13
Orthorhombique	9
Tétragonal	7-6
Rhomboédrique	7-6
Hexagonal	5
Cubique	3

For an orthorhombic structure (the crystal structure of the herein studied materials) is characterized by nine independent elastic constants $C_{11}, C_{22}, C_{33}, C_{44}, C_{55}, C_{66}, C_{12}, C_{13}\ and\ C_{32}$; and all other constants are equal to zero. The tensor of the elastic constants is written in this case:

$$C_{ij} = \begin{pmatrix} C_{11} & C_{12} & C_{13} & 0 & 0 & 0\\ C_{12} & C_{22} & C_{23} & 0 & 0 & 0\\ C_{13} & C_{23} & C_{33} & 0 & 0 & 0\\ 0 & 0 & 0 & C_{44} & 0 & 0\\ 0 & 0 & 0 & 0 & C_{55} & 0\\ 0 & 0 & 0 & 0 & 0 & C_{66} \end{pmatrix} \qquad \text{(II.44)}$$

II.9.2 Conditions of mechanical stability

A necessary condition for mechanical stability is that the matrix of elastic constants is positively defined. The condition of mechanical stability of a cristal structure implies that the variation of internal energy under any small deformation is positive. This condition can be formulated in terms of elastic constants C_{ij}.

The mechanical stability of an orthorhombic system requires that their independent elastic constants obey the following Born conditions [26].

$$\begin{cases} C_{ii} > 0 \ (i = 1,4,5,6) \\ C_{11}C_{22} > C_{12}^2 \\ C_{11}C_{22}C_{33} + 2C_{12}C_{13}C_{23} - C_{11}C_{23}^2 - C_{22}C_{13}^2 - C_{33}C_{12}^2 > 0 \end{cases}$$

II.9.3 Polycrystalline elastic moduli

The elastic behavior of an isotropic system is fully described by the bulk modulus B and the shear modulus G (shear modulus). From these two independent elastic moduli we can define the Young's modulus E and the Poisson's coefficient υ **Table II .2**

These polycrystalline elastic moduli are calculated in the Voigt-Reuss-Hill approximation. The Voigt upper limit. correspond to average of Hooke's C_{ij} on all the possible orientations of the grains. It based on the assumption that the deformation is uniform in each grain. As for the Voigt limit, the Reuss lower limit makes an average on the inverse relationship S_{ij}, it is based on the assumption that the stress is uniform in each grain. In practice, the Hill's average of polycrystalline elastic moduli is considered. For an orthorhombic system, these modules are defined by equations in **Table II.2,** where the V and R the indices refer respectively to Voigt and Reuss. A practical estimate of true polycrystalline elastic modules is given by the Hill average:

$$B_H = (B_V + B_R)/2$$

$$G_H = (G_V + G_B)/2$$

Table II. 3: *The physical significance of each elasticitic modulus and its equation as a function of C_{ij} in the Voigt and Reuss methods approximations.*

Modules of elasticity	Physical meaning	Equation
Compressibility module	Hydrostatic pressure change resistance	$B_V = \frac{1}{9}[C_{11} + C_{22} + C_{33} + 2(C_{12} + C_{13} + C_{23})]$ $B_R = [S_{11} + S_{22} + S_{33} + 2(S_{12} + S_{13} + S_{23})]^{-1}$
Shear modulus	Resistance to the sliding motion of the planes inside the solid	$G_V = (C_{11} + C_{22} + C_{33}) - (C_{12} + C_{13} + C_{23}) + 3(C_{44} + C_{55} + C_{66})$ $15G_R = 4(S_{11} + S_{22} + S_{33} - S_{12} - S_{13} - S_{23}) + 3(S_{44} + S_{55} + S_{66})$
Young's module	Resistance to uni-axial deformation	$E = \frac{9BG}{3B + G}$
Poisson coefficient	Characterizes the contraction of matter perpendicular to the direction of applied effort.	$\upsilon = \frac{3B - 2G}{2(3B + G)}$
Vickers hardness Chens's model [27]	Defined as the resistance of a material to various types of deformations.	$H_V = 0.1475.G$

Where V, R the indices refer respectively to Voigt, Reuss. A practical estimate of true polycrystalline elastic modules is given by the Hill average: $B_H = (B_V + B_R)/2$ and

$G_H = (G_V + G_B)/2$

II.9.4 Anisotropy of elastic behavior

The elastic anisotropy is mechanically translated by a dependence of the elastic response of a crystalline material versus the direction of stress. It is defined in our study by four different approaches:

Table II. 4: *The physical meaning of each anisotropy index and its corresponding equation.*

Indices of anisotropy	Equation	Physical meaning
The universal anisotropy index	$A^U = 5\frac{G_V}{G_R} + \frac{B_V}{B_R} - 6$	For an isotropic system A^U=0, while any deviation from zero indicates the degree of anisotropy.
Percentage of anisotropy in compressibility	$A_B = \frac{B_V - B_R}{B_V + B_R} \times 100$	0% indicates isotropic behavior, while of all deviation from the extent of elastic anisotropy.
Percentage of shear anisotropy	$A_G = \frac{G_V - G_R}{G_V + G_R} \times 100$	
Coefficients of anisotropies in shear	$A_1 = \frac{4C_{44}}{C_{11} + C_{33} - 2C_{13}}$ $A_2 = \frac{4C_{55}}{C_{22} + C_{33} - 2C_{23}}$ $A_3 = \frac{4C_{66}}{C_{11} + C_{22} - 2C_{12}}$	The degree of shear anisotropy can be identified by the deviation of these coefficients of unity.

Or A_1 the shear anisotropy coefficient for the plans {100} between the management ⟨011⟩ and ⟨010⟩, A_2 is the coefficient of shear anisotropy for the plans{010} between directions ⟨101⟩ and ⟨001⟩, and A_3 is the coefficient of shear anisotropy for the plans {001} between directions ⟨110⟩ and ⟨010⟩.

Another useful and more direct way to identify elastic anisotropy is to graph a three-dimensional surface diagram of the directional dependence of the elastic modules. Each point of this surface is identified by its position vector whose module represents the value of the elastic quantity measured in the direction given by the direction cosines in spherical coordinates of this vector. The directional dependence of Young's modulus and bulk modulus for an orthorhombic crystal is given by **[28]**:

$$E = [S_{11}l_1^4 + S_{22}l_2^4 + S_{33}l_3^4 + (2S_{13} + S_{55})l_1^2l_3^2 + (2S_{12} + S_{66})l_1^2l_2^2 + (2S_{23} + S_{44})l_2^2l_3^2]^{-1} \quad \text{(II.46)}$$

$$B = [(S_{11} + S_{12} + S_{13})l_1^2 + (S_{12} + S_{22} + S_{23})l_2^2 + (S_{13} + S_{23} + S_{33})l_3^2]^{-1} \quad \text{(II.47)}$$

where S_{ij} are the compliance constants of the material, and l_i are direction cosines of direction respectively given in spherical coordinates by:

$$\begin{cases} l_1 = cos(\varphi)sin(\theta) \\ l_2 = sin(\varphi)sin(\theta) \\ l_3 = cos(\theta) \end{cases} \quad \text{(II.48)}$$

A perfect spherical shape indicates an isotropic behavior. Yet, any deviation from the sphericity indicates a certain degree of anisotropy.

II.9.5 Debye temperature and elastic wave velocities

One of the most important parameters that determines the thermodynamic properties of materials is the Debye temperature. By definition, it is the temperature at which the vibrations of the atoms in the solid reach their maximum of possible modes. At low temperature, the Debye temperature can be derived from the average acoustic wave velocities, which are connected in turn to the elastic moduli via the following equations:

$$\theta_D = \frac{h}{K_B}\left[\frac{3n}{4\pi}\left(\frac{\rho N_A}{M}\right)\right]^{1/3} V_M \quad \text{(II.49)}$$

$$V_M = \left[\frac{1}{3}\left(\frac{2}{V_t^3} + \frac{1}{V_L^3}\right)\right]^{-1/3} \quad \text{(II.50)}$$

$$V_t = \left(\frac{G}{\rho}\right)^{1/2} \quad \text{(II.51)}$$

$$V_l = \left(\frac{3B+4G}{3\rho}\right)^{1/2} \quad \text{(II.52)}$$

Where h is the Planck constant, K_B is the Boltzmann constant, n is the number of atoms per molecule, N_A is the Avogadro number, ρ is the density of the material, and M is is the molecular weight. V_M , V_l and V_t are respectively the average, longitudinal and transverse acoustic wave velocities.

II.10 Optical properties

Optics is the field of physics that describes luminous phenomena. It is of great interest to know the different ways in which light interacts with matter in solid state physics, for example absorption, transmission, reflection, diffusion and emission. The study of the optical properties of solids has proven to be a powerful tool in our understanding of the electronic properties of materials.

II.10.1 The dielectric function

The dielectric function of a material $\varepsilon(\omega, k)$ describes its optical response when it is subjected to the oscillating electric field of an electromagnetic wave. This physical quantity depends substantially on the structure of the energy bands of the material considered and it is determined

by the electronic transitions between the valence bands and the conduction bands. It consists of a real part and another imaginary part, and it is given by [29].

$$\varepsilon(\omega) = \varepsilon_1(\omega) + i\varepsilon_2(\omega) \quad \text{(II.53)}$$

In reality, the two real parts $\varepsilon_1(\omega)$and imaginary $\varepsilon_2(\omega)$ of the dielectric function are not independent of each other. Indeed, each can be deduced knowing the other by using the Kramers-Kronig relation [30].

$$\varepsilon_1(\omega) = 1 + \frac{2}{\pi} P \int_0^{\infty} \frac{\omega \varepsilon_2(\dot{\omega})}{(\dot{\omega})^2 - \omega^2} d\dot{\omega} \quad \text{(II.54)}$$

$$\varepsilon_2(\omega) = -\frac{2}{\pi} P \int_0^{\infty} \frac{\varepsilon_1(\dot{\omega}) - 1}{(\dot{\omega})^2 - \omega^2} d\dot{\omega} \quad \text{(II.55)}$$

Where ω is the frequency and P is the main part of the Cauchy integral.

II.10.2 The refractive index

The refractive index $n(\omega)$ of a material is defined by the ratio of the speed of light in the vacuum c to the speed of light in the material v according to:

$$n = \frac{c}{v} \quad \text{(II.55)}$$

The refraction of a medium can be described by a single quantity called the complex refractive index. It is usually represented by the symbol $\tilde{n}$ defined by the equation:

$$\tilde{n} = n + ik \quad \text{(II.56)}$$

The real part of $\tilde{n}$, namely n, is the same as the index of refraction at normal incidence. The imaginary part of n, namely k, is called the extinction coefficient. Both Quantities are related to the dielectric function by the following two relations [31]:

$$n(\omega) = \frac{1}{\sqrt{2}} \left[\sqrt{\varepsilon_1^2(\omega) + \varepsilon_2^2(\omega)} + \varepsilon_1(\omega) \right]^{1/2} \quad \text{(II.57)}$$

$$k(\omega) = \frac{1}{\sqrt{2}} \left[\sqrt{\varepsilon_1^2(\omega) + \varepsilon_2^2(\omega)} - \varepsilon_1(\omega) \right]^{1/2} \quad \text{(II.58)}$$

II.10.3 The absorption coefficient

The absorption coefficient $\alpha(\omega)$indicates the fraction of the energy lost by the wave as it passes through the material. It can be defined according to the extinction coefficient $k(\omega)$ by the following relation [32]:

$$\alpha(\omega) = \frac{4\pi}{\lambda} k(\omega) \quad \text{(II.59)}$$

Where λ represents the wavelength of light in a vacuum.

II.10.4 Reflectivity

The reflection of radiation on a surface is described by the reflection coefficient or reflectivity. This is usually designated by the symbol $R(\omega)$and is defined like the ratio of the reflected intensity to the incident intensity on the surface **[33],** this property defines the colors of the metals. The reflectivity is calculated from the index of refraction and extinction coefficient by the following relation **[31]**:

$$R(\omega) = \frac{n+ik-1}{n+ik+1} \quad \text{(II.60)}$$

Conclusion

In this chapter, we give a brief description of the few concepts and methods adopted in this study. Of particular attention, an overview is given on the density functional theory (DFT), and on the elastic and optical properties of crystalline materials. DFT is based on Hohenberg and Kohn's theorem, and it asserts that all the physical properties of the ground state of an electron gas depend only on its density. The formalism of Kohn and Sham makes it possible to take advantage of this theorem and calculate the total energy of an electron system. The two most used methods in the construction of the wave function and therefore the electronic density are the pseudopotential (PP) method and the plane wave (PP) method. We have exposed here three approximations used in the practical calculations of the exchange-correlation energy namely, the approximation of hybrid functions, the generalized gradient (GGA) approximation and the local density approximation (LDA). Moreover, an over view of the CASTEP code is given.

Bibliographical references

1. Schrödinger, E., *Quantisierung als eigenwertproblem.* Annalen der physik, 1926. **385**(13): p. 437-490.
2. Born, M. and J.R. Oppenheimer, *On the quantum theory of molecules.* Сборник статей к мультимедийному электронному учебно-методическому комплексу по дисциплине «физика атома и атомных явлений»/отв. ред. Шундалов МБ; БГУ, Физический факультет, 1927.
3. Hartree, D.R. *The wave mechanics of an atom with a non-Coulomb central field. Part I. Theory and methods*. in *Mathematical Proceedings of the Cambridge Philosophical Society*. 1928. Cambridge University Press.
4. Martin, R.M., *Electronic structure: basic theory and practical methods*. 2004: Cambridge university press.
5. Thomas, L.H. *The calculation of atomic fields*. in *Mathematical Proceedings of the Cambridge Philosophical Society*. 1927. Cambridge University Press.
6. Fermi, E., *Un metodo statistico per la determinazione di alcune priorieta dell'atome.* Rend. Accad. Naz. Lincei, 1927. **6**(602-607): p. 32.
7. Schrödinger, E., *An Undulatory Theory of the Mechanics of Atoms and Molecules.* Physical Review, 1926. **28**(6): p. 1049-1070.
8. Dirac, P.A. *Note on exchange phenomena in the Thomas atom*. in *Mathematical Proceedings of the Cambridge Philosophical Society*. 1930. Cambridge University Press.
9. Hohenberg, P. and W. Kohn, *Inhomogeneous Electron Gas Physical Review 136.* B864, 1964.
10. Ceperley, D.M. and B. Alder, *Ground state of the electron gas by a stochastic method.* Physical Review Letters, 1980. **45**(7): p. 566.
11. Combelles, C., *Modélisation ab-initio Appliquée à la Conception de Nouvelles Batteries Li-Ion*. 2009, Université Montpellier II-Sciences et Techniques du Languedoc.
12. Becke, A.D., *Density-functional exchange-energy approximation with correct asymptotic behavior.* Physical Review A, 1988. **38**(6): p. 3098-3100.
13. Perdew, J.P., *Unified theory of exchange and correlation beyond the local density approximation.* Electronic structure of solids' 91, 1991. **11**.
14. Perdew, J.P., K. Burke, and M. Ernzerhof, *Generalized gradient approximation made simple.* Physical review letters, 1996. **77**(18): p. 3865.
15. Hammer, B., L.B. Hansen, and J.K. Nørskov, *Improved adsorption energetics within density-functional theory using revised Perdew-Burke-Ernzerhof functionals.* Physical Review B, 1999. **59**(11): p. 7413.
16. Wahl, R., D. Vogtenhuber, and G. Kresse, *SrTiO 3 and BaTiO 3 revisited using the projector augmented wave method: Performance of hybrid and semilocal functionals.* Physical Review B, 2008. **78**(10): p. 104116.
17. DADDA, N., *Composés Hybrides: Synthèse, Structure, Topologie et Densité Electronique des Liaisons Hydrogène*. 2013, Université de Constantine 1.
18. Kiréev, P., *La physique des semiconducteurs. 2e édition, édition Mir*. 1975, Moscou.
19. Makov, G., R. Shah, and M. Payne, *Periodic boundary conditions in ab initio calculations. II. Brillouin-zone sampling for aperiodic systems.* Physical Review B, 1996. **53**(23): p. 15513.

20. Khadidja, D., *Propriétés électroniques et élastiques des semiconducteurs anorganiques*. 2012, Université de Sétif 1-Ferhat Abbas.
21. Nassim, M.A., *ÉTUDE ab-initio DES DÉFAUTS INTRINSÈQUES DANS LES MATÉRIAUX CHALCOPYRITES Cu-III-S2*. 2012, Université de Laghouat-Amar Telidji.
22. Vanderbilt, D., *Soft self-consistent pseudopotentials in a generalized eigenvalue formalism.* Physical review B, 1990. **41**(11): p. 7892.
23. Segall, M., et al., *First-principles simulation: ideas, illustrations and the CASTEP code.* Journal of Physics: Condensed Matter, 2002. **14**(11): p. 2717.
24. Payne, M.C., et al., *Iterative minimization techniques for ab initio total-energy calculations: molecular dynamics and conjugate gradients.* Reviews of modern physics, 1992. **64**(4): p. 1045.
25. Monkhorst, H.J. and J.D. Pack, *Special points for Brillouin-zone integrations.* Physical Review B, 1976. **13**(12): p. 5188-5192.
26. Mouhat, F. and F.-X. Coudert, *Necessary and sufficient elastic stability conditions in various crystal systems.* Physical Review B, 2014. **90**(22): p. 224104.
27. Guechi, A., et al., *Pressure effect on the structural, elastic, electronic and optical properties of the Zintl phase KAsSn, first principles study.* Journal of Alloys and Compounds, 2015. **623**: p. 219-228.
28. Nye, J.F., *Physical properties of crystals: their representation by tensors and matrices*. 1985: Oxford university press.
29. Hosseini, S., T. Movlarooy, and A. Kompany, *First-principles study of the optical properties of $PbTiO_3$*. The European Physical Journal B-Condensed Matter and Complex Systems, 2005. **46**(4): p. 463-469.
30. *F. Wooten: Optical Properties of Solids, Academic Press, New York and London, 1972,*
31. Saha, S., T. Sinha, and A. Mookerjee, *Structural and optical properties of paraelectric SrTiO3.* Journal of Physics: Condensed Matter, 2000. **12**(14): p. 3325.
32. Goubin, F., *Relation entre fonction diélectrique et propriétés optiques: application à la recherche d'absorbeurs UV inorganiques de deuxième génération*. 2003, Université de Nantes.
33. Dupeux, M., *AIDE-MEMOIRE SCIENCE DES MATERIAUX,© Dunod.* 2004.

Chapitre III
Résultats et discussion

III.1 Introduction

In this chapter, we will present the results for the optimized structural parameters and the predicted elastic and electronic properties for the orthorhombic polar intermetallic compounds Na_2CuPn $(Pn = As, P)$.

III.2 Calculation details

All calculations conducted in the present work were performed using CASTEP code [1] based on the pseudo-potential [2] and plane waves schemes (PP-PW) of DFT theory. We make use of Generalized Gradient Approximation (GGA) as parameterized by Perdew-Burk-Ernzerhof "PBE". Electron-ionic interactions were treated by on-the-fly generated ultra-soft pseudopotentials (OTFG-USPP) [2]. For an accurate prediction of the subsequent key physical properties, scaler relativistic effect have been considered in the generation of the pseudo potential using the technic proposed by Koelling and Hamon [3]. Valence states were modelled by ($2s^2 2p^6 3s^1$) for Na, ($3d^{10} 4s^1$) for Cu, ($3d^{10} 4s^2 4p^3$) for As and ($3s^2 3p^3$) for P. In a DFT calculation, the physical properties of a system are functional of the electron density of the ground state. This density is the one that minimizes the total energy of the system. It is therefore imperative to express this energy with the greatest possible precision. In order to ensure convergence of the computed structures and energy, the parameters that affect the calculation accuracy were selected after performing careful convergence tests. The self-consistent loop was iterated until the total energy difference of the system between the consecutive iterating steps becomes less than 10^{-6} eV/atom. First, the Cutoff energy (E_{cut}) convergence study has been performed, than convergence with respect to Brillouin zone sampling has been conducted, the results are reported in the next section.

III.3 Convergence study

First, it is necessary to optimize the calculation parameters before proceeding to the calculation of the different properties. That is to say, for the pseudo-potential and plane wave method, it is a matter of optimizing the size of the plane wave basis set on which the orbitals of Kohn and Sham are expressed, and the number of points k $(nkpt)$ used for integration in the irreducible Brillouin zone.

III.3.1. Choice of the size of the plane wave basis set

Kohn-Sham orbitals are decomposed on a plane wave basis set. However, this decomposition is only accurate if this basis is infinite, this is practically impossible. Consequently, these basis are often truncated by the value of the kinetic energy of the plane wave whose frequency is the highest. This energy is called cutoff energy E_{cut}, which is responsible for the size of the basis set on which the electronic wave function is projected. We can consider that the basis size is sufficient when the total energy as a function of the cutoff energy reaches a standing value; therefore, we say that the total energy is converged.

For the Na_2CuPn polar compounds ($Pn = As, P$), the converged total energy is obtained for a cut-off energy $E_{cut} = 700\,eV$. The results of the convergence study of total energy as a function of E_{cut} for these compounds are shown in **Figure III.1**

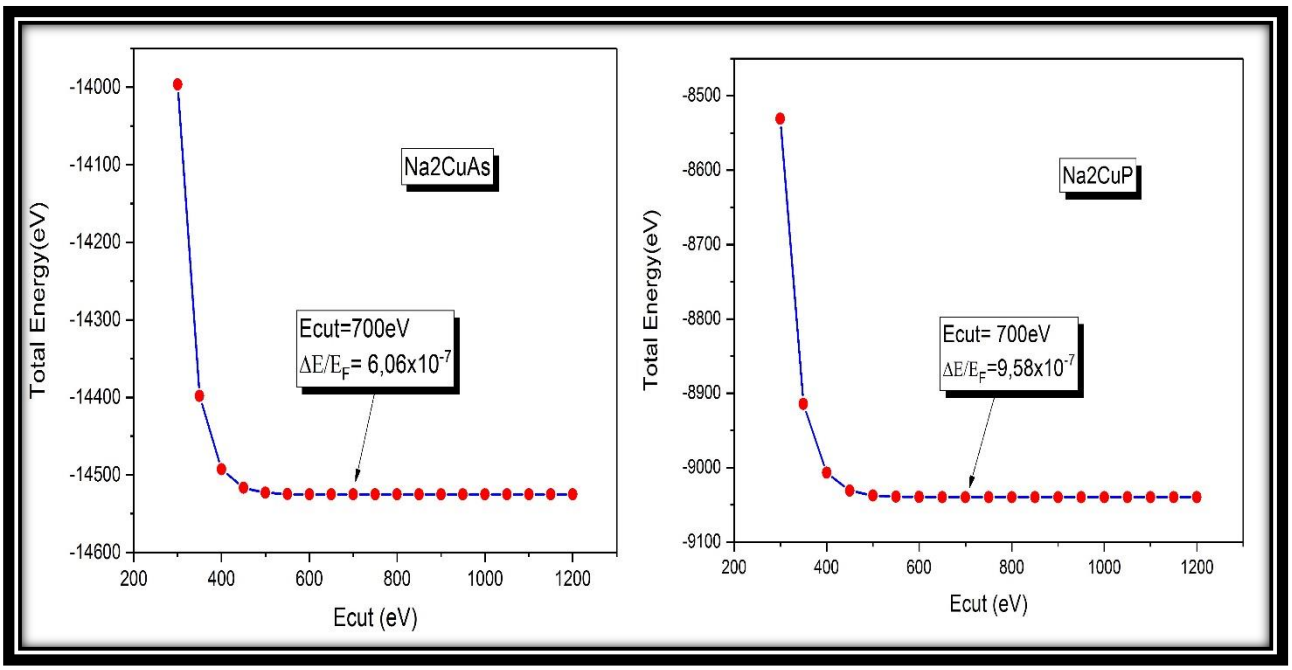

Figure III.1: *Convergence of the total energy as a function of* E_{cut} *for compounds* Na_2CuPn $(Pn = As, P)$

The most important criterion in this study is the relative variation of the total energy as a function of E_{cut}, **Table III.1** shows the evolution of E_{tot} as a function of E_{cut} for Na_2CuAs.

***Table III.1**: Convergence of total energy as a function of E_{cut} for Na_2CuAs with the relative variation of energy, E_F is the final energy corresponding to the highest cut-off energy*

Na_2CuAs		
E_{cut} *(eV)*	*Total Energy (eV)*	$\Delta E/E_F$
300	-13996,5958	0,03639270583
350	- 14398,1810	0,0087452383
400	- 14492,6454	0,00224175801
450	- 14516,6332	5,90297939567E-4
500	- 14522,9972	1,52163059648E-4
550	- 14524,6625	3,7514094291E-5
600	- 14525,0967	7,62123369061E-6
650	- 14525,1863	1,45264707201E-6
700	**- 14525,1986**	**6,05843328612E-7**
750	- 14525,1993	5,57651245655E-7
800	- 14525,2008	4,54382496459E-7
850	- 14525,2028	3,16690830866E-7
900	- 14525,2043	2,1342208167E-7
950	-14525,2050	1,65229998712E-7
1000	-14525,2052	1,51460855093E-7
1050	- 14525,2053	1,44576248873E-7
1100	- 14525,2057	1,17037915755E-7
1150	- 14525,2064	6,88458327969E-8
1200	- 14525,2074	0

As can be see from **Table III.1**, the relative variation of the total energy is of the order of 10^{-7} at $E_{cut} = 700\ eV$.

III.3.2. Brillouin Zone (BZ) Sampling

In order to obtain properties such as total energy, charge density, etc., it is imperative to integrate on k points in the Brillouin zone. The computation is necessarily carried out on a discrete set of relevant k point to correctly present the fictitious states in reciprocal space.

With the CASTEP code, the integral on the first BZ is approximated by a discrete (finite) sum over a special set of k points using the standard method of Monkhorst and Pack [4]. After determining the cutoff energy, it is set at its optimum value and the number of k points is varied. For each of these values, the total energy is calculated. It is said that the total energy is converged with respect to the number of k points when the total energy reaches a standing value.

For theNa_2CuPn polar compounds ($Pn = As, P$), the total converged energy is obtained for a $7 \times 7 \times 7$ sampling grid of the irreducible Brillouin zone, this gives a relative variation of

the total energy of the order of 10^{-7}. **Figure III.2** shows the results of this study, and **Table III.2** provides an overview of the evolution of E_{tot} versus $Nkpt$ for Na_2CuAs.

Table III.2: *Convergence of total energy as function of k points, for Na2CuAs* $(E_{cut} = 700eV)$, E_F *is the final energy corresponding to the most dense Brillioin zone sampling.*

Na2CuAs		
K-points	*Total Energy (eV)*	$\Delta E/E_F$
2x2x2	-14526,1336	-1,76374888033E-5
3x3x3	-14525,8123	4,48165699099E-6
4x4x4	-14525,8940	-1,14278811137E-6
4x4x5	-14525,8720	3,71750349483E-7
5x5x5	-14525,8714	4,1305594387E-7
6x6x6	-14525,8799	-1,72106643279E-7
6x6x7	-14525,8766	5,50741258494E-8
7x7x7	**-14525,8766**	**5,50741258494E-8**
8x8x8	-14525,8780	-4,1305594387E-8
8x8x9	-14525,87741848	-5,71394054993E-11
9x9x9	-14525,87741765	0

The convergence tests for the two studied compounds, allow us to choose as calculation parameters the values: $E_{cut} = 700\ eV$ and a grid of $7 \times 7 \times 7$. The choice of these settings can be used to optimize the accuracy based on available computing resources.

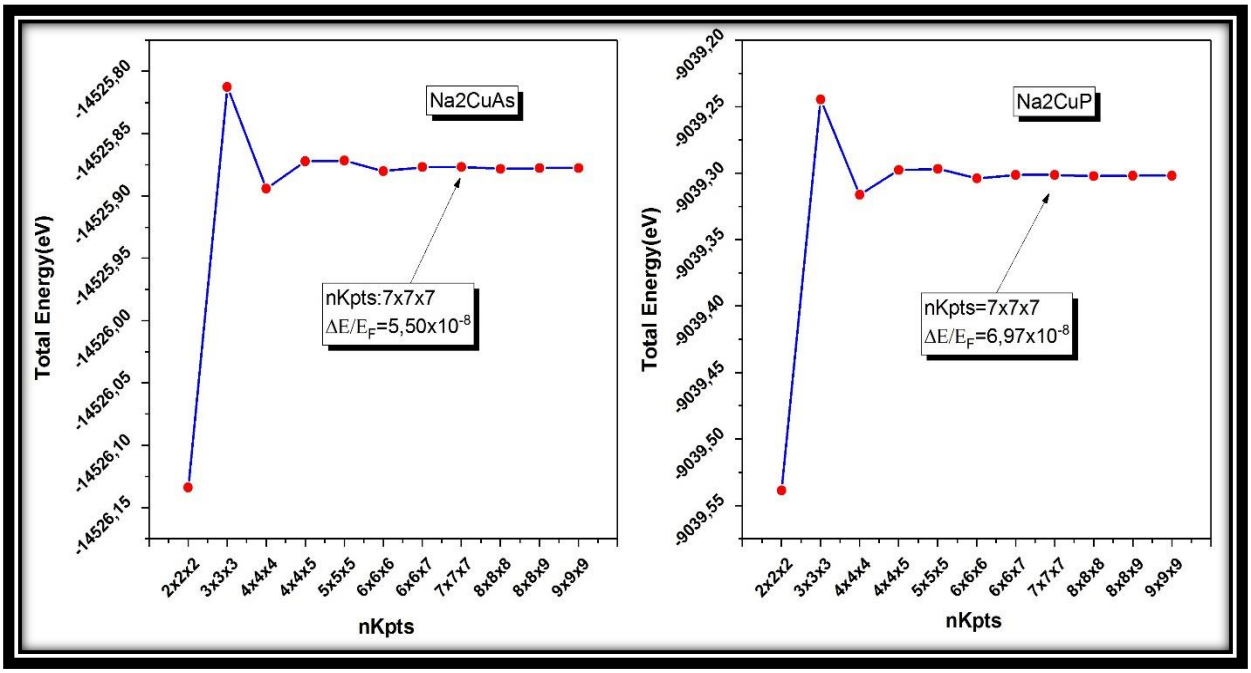

Figure III.2*: Convergence of the total energy as a function of nKpts for compounds* (Na_2CuAs, *and* Na_2CuP).

III.4 Structural properties

To determine the different properties of the ground state, it is important, first of all to proceed with the optimization of the equilibrium geometry of the studied system. This step allows us to obtain a relaxed structure which corresponds to a minimum of total energy. This consists in canceling Hellmann-Feynman's forces [5, 6] , which are exerted on the atoms of the solid.

We fisrt start to verify whether the selected calculation parameters reproduce the experimental ground state geometry. The bulk Na_2CuP [7], Na_2CuAs [8] structures were used for the subsequent tight optimizations. The total energy was minimized self consistently using the Broyden-Fletcher-Goldfarb-Shanno algorithm (BFGS) [9-13] . Both lattice parameters and atomic positions were fully relaxed, respecting the following convergence criteria:

- Tolerance in energy: $5.0 \times 10^{-6}\ eV/atom$.
- Max force : $0.01\ eV/$Å.
- Max stress : $0.02\ GPa$.
- Max displacement : 5.0×10^{-4}Å.

The obtained results including the ground state equilibrium structural parameters, atomic coordinates, cell volumes and density of the herein considered materials are represented in **Tables III.3** and **4** alongside the available experimental data [7, 8] for comparison.

***Table III.3**: calculated (Cal) and Experimental (Exp) structural parameters: cell parameters (a, b and c), volume (V), and density (ρ) for Na_2CuPn ($Pn = As, P$).*

System	Na_2CuP			Na_2CuAs		
Chemical name	Copper (I) Disodium Phosphide			Copper Sodium Arsenide		
Space group, Z	Cmcm (No.63), 4			Cmcm (No.63), 4		
Symmetry	Orthorhombic			Orthorhombic		
	Cal.	**Exp. [7]**	**d (%)**	**Cal.**	**Exp.[8]**	**d (%)**
Unit cell parameters (Å)	$a = 8{,}72$	$a = 8.67$	$+0.576$	$a = 8.92$	$a = 8.86$	$+0.677$
	$b = 6.96$	$b = 6.98$	-0.286	$b = 7.20$	$b = 7.22$	-0.277
	$c = 5.26$	$c = 5.30$	-0.754	$c = 5.35$	$c = 5.34$	$+0.187$
a/c	1.658	1.636	$+1.614$	1.667	1.659	$+0.482$
b/c	1.323	1.317	$+0.455$	1.346	1.352	-0.443
Cell volume (Å^3)	319,339	320.74	-0.436	343,326	341.6	$+0.505$
Density (g/cm^3)	2,92236	2,90961	$+1,275$	3,56842	3,58650	-0.504

***Table III.4**: calculated (Cal) and Experimental (Exp) atomic coordinates (x, y, z) (for Na_2CuPn $(Pn = As, P)$, and Wyckoff position (P.W).*

	Atom	W. P.	X		Y		Z	
			Cal.	Exp.	Cal.	Exp.	Cal.	Exp.
Na_2CuP	Na_2	$8g$	0.32624	0.3273^a	0.35767	0.3588^a	0.25	0.25
	Cu	$4b$	0.5	0.5	0	0	0	0
	P	$4c$	0	0	0.26853	0.2405^a	0.25	0.25
Na_2CuAs	Na_2	$8g$	0.32485	0.3262^b	0.35407	0.3559^b	0.25	0.25
	Cu	$4b$	0	0	0.5	0.5	0	0
	As	$4c$	0	0	0.23120	0.2343^b	0.25	0.25

[a] Ref.[7]

[b] Ref.[8]

As can be clearly seen from, **Table *III.3*** and ***4,*** the obtained equilibrium structural parameters including unit cell lattice parameters, atomic coordinates, cell volume and density are in excellent agreement with their experimental counterpart. The good agreement between our calculated results and the available experimental data demonstrates the reliability of the computational methodology adapted here and gives confidence on the subsequent calculated electronic, elastic and optical properties reported in the next sections. Remarkably, going down the periodic table from P to As , the calculated cell volume and lattices parameters are increased. This can be explained by the increased atomic radii of the considered atomic spices.

III.5. Elastic Properties

The elastic properties are intimately correlated with many fundamental physical properties, including key thermodynamic properties such as: Debye temperature, heat capacity, sound velocity, phonon frequencies, heat conductivity…

The analysis of the elastic behavior of a material is reduced to the determination of the corresponding elastic constants (stiffness tensor) C_{ij}. Then, the anisotropy of the interatomic bonds, the mechanical, vibrational and thermodynamic properties are accessed by the simple knowledge of the elastic constants C_{ij}, these parameters can be determined efficiently from the ab initio calculations.

In this section, the computed complete set of elastic stiffness constants of the considered polar intermetallic compounds will be used to characterize their mechanical behavior. To the

best of our knowledge, neither experimental nor theoretical data are available in the literature to be compared to our results.

III.5.1. Elastic stiffness constants

For the considered orthorhombic crystal structures, the nine elastic constants, namely: C_{11}, C_{22}, C_{33}, C_{44}, C_{55}, C_{66}, C_{12}, C_{13}, C_{23}, are calculated using the static strain technic **[14]**. A symmetry unique strain is applied, and the resultant stress is calculated using the following convergence criteria:

- Energy tolerance : $10^{-6}\ eV/atom$.
- Maximum forces : 0,002 $eV/$Å.
- Maximum displacement: 1.0×10^{-4} Å.

The obtained results are summarized on ***Table III.5***.

Table III.5: *Calculated elastic stiffness coefficients (C_{ij}, in GPa) of the Na_2CuPn ($Pn = As, P$) compounds.*

	C_{11}	C_{22}	C_{33}	C_{44}	C_{55}	C_{66}	C_{12}	C_{13}	C_{23}
Na_2CuP	61.43	76.69	52.92	36.92	13.38	11.85	4.64	−5.85	30.93
Na_2CuAs	65.40	67.83	55.97	33.52	13.31	9.31	10.62	6.20	32.34

From ***Table III.5*** it is obvious that the elastic constants C_{ii} $(i = 1 \ldots 3)$, are larger than the other elastic constants, giving evidence that the considered compounds are more resistant to compressional deformation than to shear distortions. Besides, since $C_{22} > C_{11} > C_{33}$, it can be concluded that the b-axe is the most incompressible, and the c axe is soft and easily compressible.

III.5.2. Mechanical stability

For a crystal to be mechanically stable, the strain energy must be positive. This means for an orthorhombic crystal that the complete set of elastic constants C_{ij} must fulfil the following born stability criteria **[15, 16]**.

$$\begin{cases} C_{ii} > 0 \ (i = 1,4,5,6) \\ C_{11}C_{22} > C_{12}^2 \\ C_{11}C_{22}C_{33} + 2C_{12}C_{13}C_{23} - C_{11}C_{23}^2 - C_{22}C_{13}^2 - C_{33}C_{12}^2 > 0 \end{cases}$$

Analysis of the calculated elestic stiffness constants show that the aformentioned creteria are verefied, confirming the mechanical stabilty of the herein considered compounds.

III.5.3. Polycristaline elastic moduli

The calculation of the latter elastic constants makes it possible to get accurate numerical estimations of other polycrystalline elastic moduli such as Young's modulus, shear modulus and Poisson's coefficient (see ***Table II.3***). The obtained results following the Voigt-Reuss-Hill approximation for Na_2CuAs and Na_2CuP are summarized in ***Table III.6***. In this approach, the Voigt **[17]** (denoted V in index) and Reuss **[18]** (denoted R) moduli are the lower and upper bounds of *B* and *G*, while the Hill **[19]** (denoted H) gives the means between the two limits (see chapter II for more details).

Actually, both of Na_2CuAs and Na_2CuP are characterized by low values of bulk modulus (*B*), suggesting that these materials are soft and easily compressible. The somewhat lower values of *G* indicates weaker ability to withstand shear strain, implying that the parameters limiting the mechanical stability of these materials is the shear modulus *G*. Furthermore, as can be seen from **Table III.6**, the values of Young's moduli *E* of the tow materials are small. This confirms that these materials have weak stiffness. A weak hardness can be expected from the aforementioned results and this is confirmed by the low values of the numerical estimate of Vickers hardness from Chens's model **[20]**.

According to Pugh's criterion **[21]**, (B/G) of polycrystalline, phases could be used to predicate the brittle $(B/G < 1.75)$ and ductile $(B/G > 1.75)$ behaviors. In light of the Pugh's viewpoint, both of the herein considered materials must be classified as fragile.

Table III.6: *Calculated bulk modulus (B, in GPa), shear modulus (G, in GPa), Young's modulus (E, in GPa), B/G ratio, Poisson ratio υ and vckers hardness (H,in GPa). The subscripts V, R and H stand to Voigt, Reuss and Hill approximations, respectively.*

	B_R	B_V	B	G_R	G_V	G	B/G	E	υ	H
Na_2CuP	24.73	27.83	26.28	17.97	23.19	20.58	1.28	48.9	0.19	3.04
Na_2CuAs	30.98	31.95	31.46	15.98	20.56	18.27	1.72	45.9	0.26	2.70

Many phenomena in the deformation of elastic materials depend on the Poisson's ratio. The simplest is that a material with a negative Poisson's ratio will get fatter in cross section when stretched and thinner when compressed. As the value of Poisson's ratio approaches 0.5, as with the rubber like materials, the material easily undergoes shear deformations but resists volumetric deformation and becomes incompressible **[22]**. The typical υ value is 0.1 for brittle covalent materials, 0.33 for ductile metallic materials and 0.25 for ionic materials, respectively.

From **Table III.6**, it can be clearly see that the Poisson's ratio of Na_2CuP is lower than 0.25 giving evidence for a more covalent bonding in this material. Meanwhile, the Poisson's ratio of

Na_2CuAs, is close to 0.25, the lower limit for ionic bonding character, suggesting a more ionic bonding in this material.

III.5.4. Elastic anisotropy

Crystal anisotropy decides atomic arrangements to follow a certain direction. Many low symmetry crystals show high extent of elastic anisotropy. Hence, it is very important to investigate anisotropic behaviors in crystal physics as well as in engineering science.

Here, we are mainly concerned with the elastic behavior of Na2CuAs and Na2CuP. Three approaches have been used.

1. First, the so called universal elastic anisotropy index A^U. A value of 0 indicates isotropic elastic behavior. While, the extent of any deviation from 0 indicates a certain degree of elastic anisotropy in both shear and compressibility. In this work, the calculated universal anisotropic indexes A^U for both compounds are greater than zero. The large deviation from zero refer to high anisotropic mechanical properties.
2. To explain the origin of this anisotropy, we have also calculated the percent anisotropy in compressibility (A_B) and shear (A_G). A value of 0% indicate a perfect isotropic medium, while the degree of any deviation from this value indicates anisotropic behavior of the considered physical property. As shown on **Table III.7**, The percent anisotropy in shear for the herein considered materials is greater than the percent anisotropy in compressibility. That is to say, elastic anisotropy in the present case arises predominantly from anisotropy in shear.
3. To gain more insights on the shear anisotropy of our compounds, we have also calculated the so called shear anisotropic factors (see **Chapter II**). Further analysis of the obtained results show that all three factors differ from unite. Meanwhile, the Shear anisotropic factor in the principal (001) plane is the more departure from unity. That is to say, the (001) shear plans are easier to be the cleavage plans among the principal plans.

Table III.7: *Calculated anisotropic indexes for the the* Na_2CuPn $(Pn = As, P)$ *compounds.*

	A^u	A_B (%)	A_G (%)	A_1	A_2	A_3
Na_2CuP	1.575	5.60	12.66	1.172	0.790	0.368
Na_2CuAs	1.466	1.53	12.55	1.230	0.900	0.333

The studies mentioned above are not enough to fully describe the anisotropy of the elastic behavior of a crystal. Another useful and more convenient way to quantify the elastic anisotropy is based on a 3D surface plot of the directional dependence of the different elastic moduli such as the Young's modulus and the bulk modulus, which are also the two most used parameters for the description of the elastic behavior of polycrystalline materials. In this illustrative picture, the

distance of a point on the surface to the origin of the coordinates system reflects the magnitude of the elastic moduli in a given direction. That is to say, a perfect isotropic medium will show a perfect spherical surface. While, any deviation from a spherical shape indicates the extant of the anisotropy of the considered elastic modulus.

For an orthorhombic crystal the directional dependence of the bulk modulus and Young's modulus can be described by the equations **II.46, II.47** (see **chapter II**). The obtained results are depicted on **Figure III.3** and **4**. From the 3D surface plot of the Young's modulus it can be concluded that both materials are large anisotropic. Meanwhile, Copper (I) Disodium Phosphide possesses the most extent of elastic anisotropy, consistent with the obtained values from universal anisotropic index. Cross sections of the 3D surface plots of Young's modulus illustrated in **Figure III.3** clearly show that the maximum value is realized when the stress is applied along the bisectors of the (bc) plan, while the minimum is realized when the stress is applied in the bisectors of the (ab) plan. As illustrated in **Figure III.4,** the bulk modulus anisotropy is less pronounced. Moreover, the b axe is the most incompressible showing good harmony with results obtained from analysis of the elastic stiffness constants.

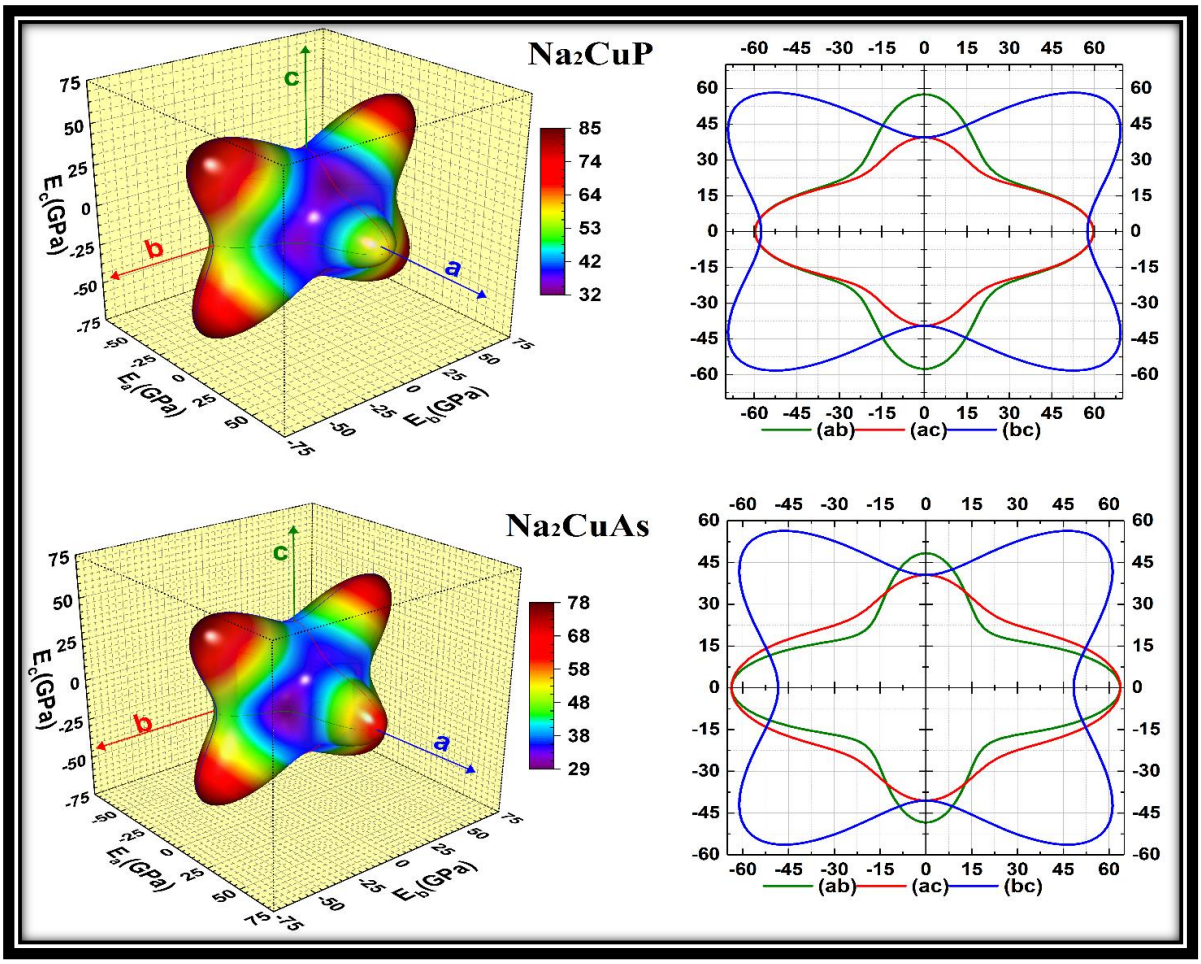

***Figure III.3**: Anisotropy of Young's modulus for (Na2CuAs and Na2CuP) compounds.*

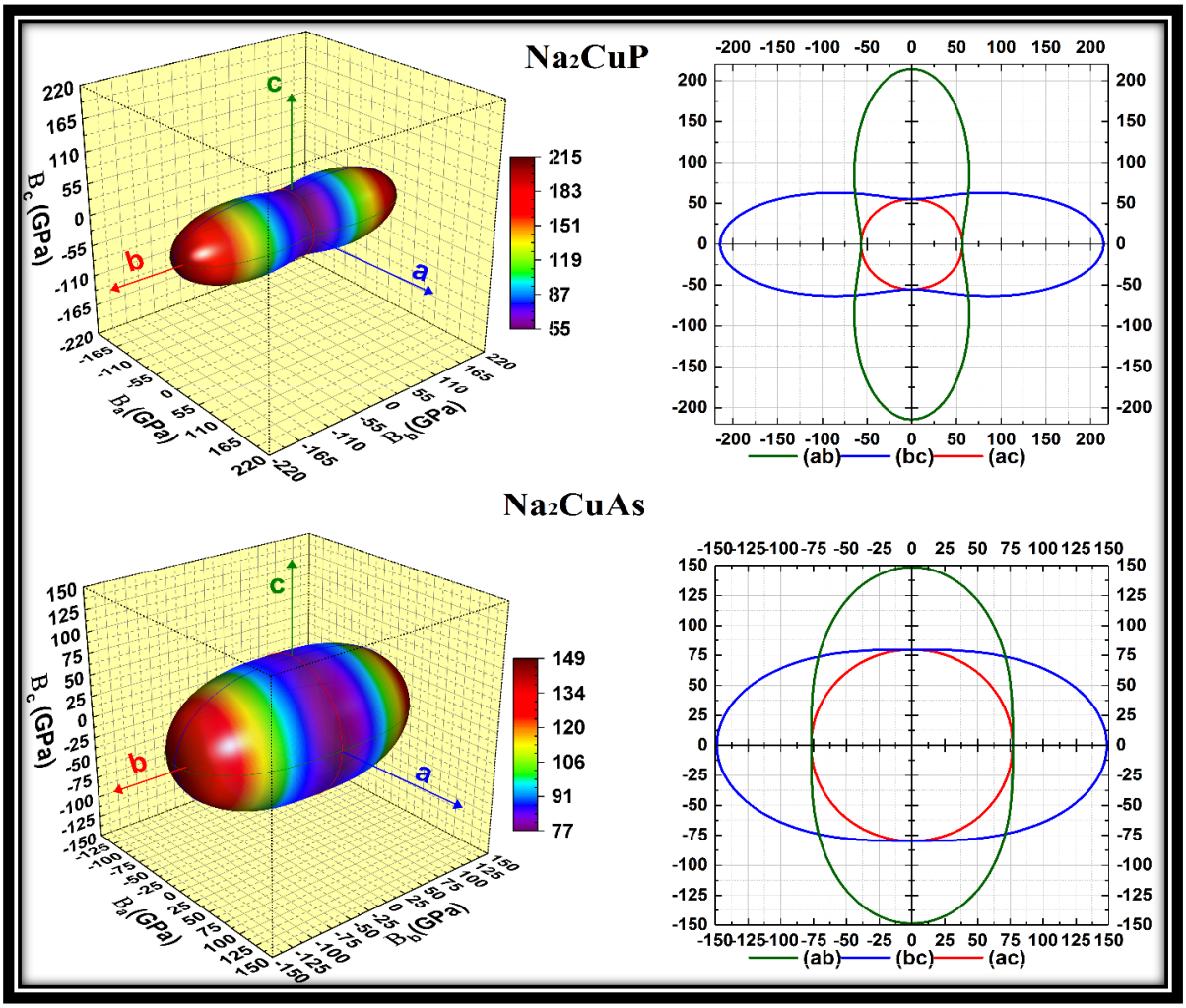

***Figure III.4**: Anisotropy of bulk modulus for (Na2CuAs and Na2CuP) compounds.*

III.5.5. Debye temperature

Debye temperature θ_D is intimately connected to various solid state phenomena such as lattice vibration, thermal conductivity, melting temperature and specific heat… ec. It reflects also strength of chemical bonding in crystalline materials. We may calculate the Debye temperature of Na_2CuAs and Na_2CuP compounds using average sound velocity V_m, the longitudinal propagation velocities v_l , transverse v_t as given by the equations (II.49,50,51,52), in chapter II. The obtained results are presented in ***Table III.8***. As can be seen from this table, both materials are characterized by low Debye temperature. The order of the calculated θ_D for our compounds is $\theta_D(Na_2CuAs) < \theta_D(Na_2CuP)$. The low Debye temperature expressed by the herein considered materials is mainly due to the low stiffness and density. Low thermal conductivity can be predicted, since at low temperatures lattice vibration are meanly due to acoustic modes.

Table III.8: *Calculated longitudinal acoustic velocities V_l (m/s), shear acoustic velocities V_s (m/s), average acoustic velocities V_m (m/s) and elastic Debye temperatures Θ_D (K) of the Na_2CuPn $(Pn = As, P)$compounds.*

	V_l	V_s	V_m	Θ
Na_2CuP	4287	2654	2926	321
Na_2CuAs	3955	2263	2514	269

III.6. Electronic Properties

The importance of the electronic properties, including the electronic band structure, total and partial density of states of a material lies in the fact that they allow us to specify its character (insulator, conductor or semiconductor), and to gain insights onto its electronic behavior. In this work, the study of the electronic properties was carried out using the GGA-PBE approximation with a denser non shifted k sampling grid of $(15 \times 15 \times 15)$ points, which corresponds to 512 points for a sampling step of 0.012 Å^{-1}.

III.6.1 Structure of the energy bands

The energy bands give the possible energies of an electron as a function of the wave vector. These bands are therefore represented in the reciprocal space, and for simplicity, only the directions between the high symmetries points in the first Brillouin zone are treated.

Figure III.5 illustrates the Brillouin zone of a representative unit cell of the herein considered polar intermetallics, along with the corresponding principal directions between the high symmetry points namely, Z(0,0,1/2), T (-1/2,1/2,1/2), Y(-1/2,1/2,0), G(0,0,0), S(0,1/2,0), R(0,1/2,1/2), Γ(0,0,1/2).

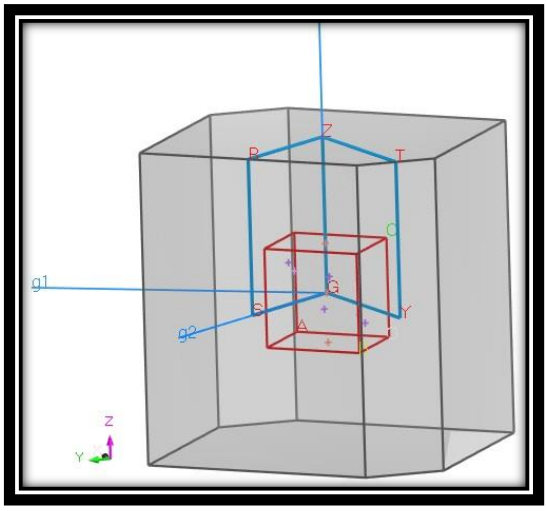

Figure III.5: *First Brillouin zone for the orthorhombic lattice* $(Cmcm)$ *and the points of high symmetry.* $(g1, g2$ *and* $g3$ *are the vectors of the reciprocal lattice*).

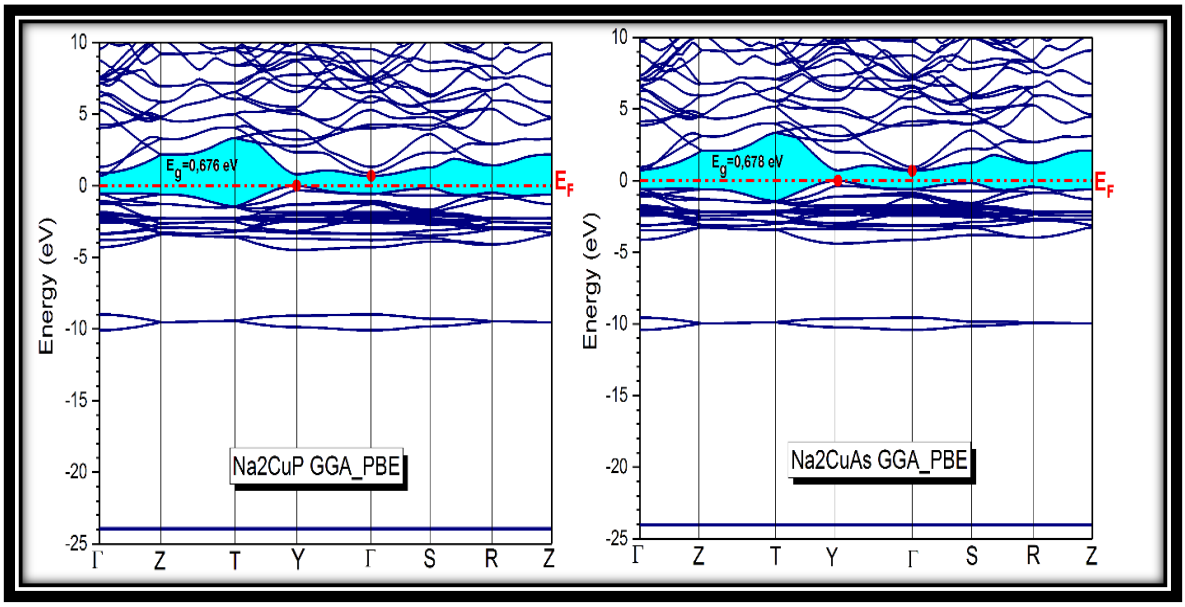

Figure III.6: *Energy band structures of Na_2CuAs; Na_2CuP calculated by GGA PBE. The Fermi level is set at 0 eV and marked by the dashed red horizontal line.*

From **Figure III.6**, it can be seen that the calculated band diagrams of the considered materials show large similarities. Moreover, the standard GGA-PBE calculations show that both materials are indirect narrow band gap semiconductors by evidence of the maximum valance band (VB) at Y , and the minimum of the conduction band (CB) at Γ. The calculated GGA-PBE band gaps are 0.678 eV and 0.676 eV for Na_2CuAs and Na_2CuP, respectevly.

In the vicinity of the Fermi level, the conduction band is meanly due to a three folds dispersed bands giving evidence for a small electronic effective mass and a good mobility. Meanwhile, at the vicinity of the valance band, the tow folded non dispersive bands give evidence of high hole effective mass. Another important character shared by the band diagrams of the considered materials is the flat and almost non dispersive bands along the Z-T, R-Z directions (perpendicular to c*) and the degenerate dispersed bands along the Z-T, R-Z, Y- Γ (parallel to c*) giving evidence that the current crystals are uniaxial.

III.6.2 Density of states

The density of states (DOS) is an important physical quantity to understand the electronic states in a material and their influence on its physical properties. Most of the electronic transport properties are determined on the basis of knowledge of the density of states. It also allows to know the nature of the chemical bonding in a material, and therefore the charge transfer between the orbitals and the atoms. From **Figure III.7**, one can clearly observe the existence of tow valleys in the valence region labeled (V1, V2). The first valley (V1) is located just bellow the Fermi level and spreads between -4.5eV and 0eV and originated predominately from an

admixture of P-3p/As-4p orbitals and Cu-3d orbitals with a small contribution from an admixture of Na-3s, Na-2p, Cu-3p, Cu-4s. Here, of special note is the strong hybridation between the Cu-3d and P-3p, which indicate covalent P-Cu interaction. The second valley (V2) which is stretched between $-10.62eV$ and $-9.35eV$ is mainly due to the confined As-4s/P-3s with a minor contribution from both Cu-4s, Cu-3p, Na-3s and Na-2p. Although, we have pointed similarities in the band structure and the electronic properties of Na_2CuAs and Na_2CuP, there is a clear difference that we have not pointed out and that deserves to be discussed. The difference can be mainly seen in the second valence band valley, which consists of a marked contribution from the Na-3s and Na-2p at V1 in Na_2CuAs than Na_2CuP.

The conduction band stem primarily from Na-3s and Na-2p with a minor contribution from both Cu-4s, Cu-3p, As-4p and As-4s, which is compatible with the assumption that the alkali metal atom donates its valance electron to form the neighboring poly-anionic $[CuPn]^{-1}$.

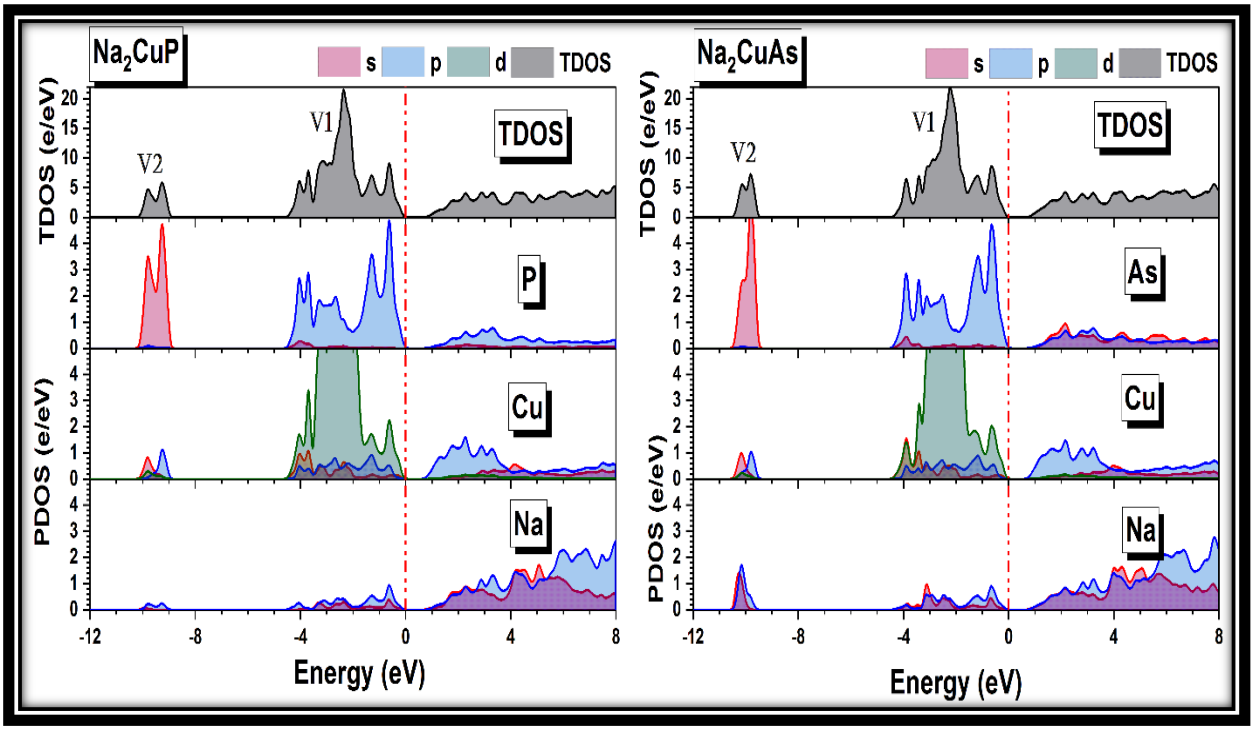

***Figure III.7**: Total and partial density of states for Na_2CuAs and Na_2CuP compounds.*

III.6.3. Mulliken population analysis

The charge density distribution is an important property of solids which provides a good description of the chemical properties. The chemical bond results from the distribution of the electronic charge between the atoms. Its behavior in a solid requires the study of the electronic charge density, which plays a central role in the determination of all the chemical and physical properties of the compound. The ionic character of a material may be related to the charge transfer between the cations and the anions. In order to gain more insights, on the charge transfer

and the chemical bonding picture of the herein considered materials, Mulliken population analysis have been performed. The obtained atomic charges are shown in **Table III.9**. It was found that $+1.3e$ $(+0.65e \times 2)$ is transferred from Na to the polyanionic unit in Na_2CuAP , while only $+0.48e$ $(+0.24e \times 2)$ is transferred in Na_2CuAs . Our results show that Na_2CuP has an average charge of $-0.68e$ per Cu and $-0.61e$ per P, while Na_2CuAs has an average charge of $-0.76e$ per Cu and +0.28e per As. Hence, the formal charges of the considered compounds are $(Na^{+0.65})_2Cu^{-0.68}P^{-0.61}$ and $(Na^{+0.24})_2Cu^{-0.76}As^{+0.28}$. To explore the charge transfers in these polar intermetallic compounds in a more straightforward way, we have also calculated the Mullikan bond populations. The obtained results are summarized in **Table III.10**. There is a clear evidence for a noticeable covalent interaction in the Cu-Cu contact along the zigzag chains, which can be clearly seen in the large positive Mulliken population (MP). Moreover, MP shows a clear difference between the two compounds. The difference can be mostly seen in the Cu-Pn contacts which have a predominant covalent character in Na_2CuP and a pure ionic nature in Na_2CuAs by evidence of the low MP. A second noticeable difference can be seen in the Na-Cu and Na-Pn interactions. Actually, from the low MP, it can be concluded that the Na-P bonds in Na_2CuP are mainly ionic in nature, however Na-As interactions in Na_2CuAs are antibonding by evidence of the negative MP.

Table III.9: *Calculated atomic effective charges fort the* Na_2CuPn $(Pn = As, P)$*compounds.*

Atom	***Na₂CuP***	***Na₂CuAs***
Na	+0.65	+0.24
Cu	-0.68	-0.76
Pn	-0.61	+0.28

Table III.10: *Interatomic distances (Å) and for the* Na_2CuPn $(Pn = As, P)$

	Bond	Distance (Å)			M. P.
		Cal.	Exp.	$\Delta d/d_{exp}(\%)$	
Na₂CuP	*Cu-P*	2.24396	2.24421[a]	+0.01	+0.76
	Cu-Cu	2.63191	2.65000[a]	+0.68	+0.52
	Na-P	2.96163	2.95539[a]	-0.21	+0.34
	Na-Cu	3.19722	3.20464[a]	+0.23	-0.26
Na₂CuAs	*Cu-As*	2.35210	2.33716[b]	-0.64	-0.05
	Cu-Cu	2.67479	2.67000[b]	-0.18	+0.77
	Na- As	3.02838	3.02054[b]	-0.26	-1.28
	Na-Cu	3.27457	3.27967[b]	+0.16	+0.14

[a] Ref. [7]

[b] Ref. [8]

III.7. optical Properties

When an electromagnetic wave of sufficient power illuminates a material, it induces electron transitions between occupied states (below E_F) and unoccupied states (above E_F). It is clear that the study of these transitions should provide some basic understanding of the electronic properties of materials.

The optical response of a material to electromagnetic radiations can be described using the frequency dependent complex dielectric function $\varepsilon(\omega)=\varepsilon_1(\omega)+i\varepsilon_2(\omega)$. The imaginary part of the dielectric function describes the absorption of the electromagnetic radiation, and can be expressed in the dipole approximation by the matrix element of transitions between the occupied valance bands and the unoccupied conduction bands by the following equation:

$$\varepsilon_2(\omega)=\frac{2\pi e^2}{m_e^2\omega^2\varepsilon_0}\sum_{c,v}\int_{BZ}\left|\left\langle\Psi_k^c\left|u.r\right|\Psi_k^v\right\rangle\right|^2\delta\left(E_k^c-E_k^v-\hbar\omega\right)dk^3 \qquad \textbf{(III.1)}$$

Where the integral is over the Brillouin zone BZ, Ψ_k^v and Ψ_k^c are the initial and finale states at *k* with their eigenvalues, *u* is the polarization vector of the incident radiation. The real part of the electric function describes the dispersion of the incident radiation in the medium. Since $\varepsilon(\omega)$ describes a causal response, $\varepsilon_1(\omega)$ can be derived from $\varepsilon_2(\omega)$ by a Kramers-Kroing transform:

$$\varepsilon_1(\omega)=1+\frac{2}{\pi}P\int_0^\infty\frac{\varpi\varepsilon_2(\omega)}{\varpi^2-\omega^2}d\varpi \qquad \textbf{(III.2)}$$

Having calculated $\varepsilon(\omega)$, many others frequency dependent optical parameters, including refractive index $n(\omega)$, extinction coefficient $k(\omega)$, absorption coefficient $\alpha(\omega)$ and the optical reflectivity $R(\omega)$ can be calculated using the following formula:

$$n(\omega)=\frac{1}{\sqrt{2}}\left[\sqrt{\varepsilon_1^2(\omega)+\varepsilon_2^2}+\varepsilon_1(\omega)\right]^{1/2} \qquad \textbf{(III.3)}$$

$$k(\omega)=\frac{1}{\sqrt{2}}\left[\sqrt{\varepsilon_1^2(\omega)+\varepsilon_2^2}-\varepsilon_1(\omega)\right]^{1/2} \qquad \textbf{(III.4)}$$

$$\alpha(\omega)=\sqrt{2}\omega\left[\sqrt{\varepsilon_1^2(\omega)+\varepsilon_2^2}-\varepsilon_1(\omega)\right]^{1/2} \qquad \textbf{(III.5)}$$

Based on the GGA-PBE calculation and using a $15 \times 15 \times 15\ k$ points non-shifted sampling mesh ($512\ k$ points) in the irreducible Brillion zone, a purely predictive study of the optical properties of the herein considered materials has been conducted. The obtained results for the key frequency dependent optical functions in the energy range [0 eV-25 eV] for polarizations parallel to the principal axes [100], [010] and [001], are depicted on **Figure III.8**.and **III.9** for Na_2CuAs and Na_2CuP respectively.

We report here that the optical response functions are identical in both directions [100] and [010], and are somewhat different in the [001] direction. So the optical properties of these materials are large anisotropic. This anisotropy disappears at higher energies.

As stated in previous text, the real part of the dielectric function $\varepsilon_1(\omega)$ describes the dispersion of the electromagnetic radiation in the medium. The obtained zero frequency dielectric constant for Na_2CuP (Na_2CuAs) is 14.58 (15.57) when $\vec{E}//[001]$ and 8.81 (9.94) when $\vec{E}//[010]$ or $\vec{E}//[100]$. Starting from the zero frequency limit, $\varepsilon_1(\omega)$ increases gradually to reach a maximum value at the lower part of the visible spectrum for polarizations along $[010]$ and $[100]$ directions, and in the IR region when $\vec{E}//[001]$. After that, $\varepsilon_1(\omega)$ decreases rapidly to reach negative values in the UV region, giving evidence for a damping of the electromagnetic radiation.

The imaginary part of the dielectric function is related to the absorption in the material. The calculated frequency dependent imaginary part of the dielectric function $\varepsilon_2(\omega)$ is depicted on **Figures III.8.b** and **III.9.h** Three well resolved peaks can be clearly seen, namely A, B and C for both materials. For Na_2CuAs (Na_2CuP), all three peaks have probably a Cu-d and As-p (P-p) character at the valance band maximum and Cu-p, Na-s and Na-p at the conduction band minimum. Due to the complexity of the band structure peculiarities at the vicinity of the Fermi level, it is difficult to allocate for each peak a specific transition.

Figures III.8.c and **III.9.i** show the variations of the reflection index as a function of the energy of the incident photons. Here, of special note.is the fairly high similarity between the $\varepsilon_1(\omega)$ and $n(\omega)$ curves. For $Na_2CuP(Na_2CuAs)$, the zero frequency refractive index $n(0)$ is predicted to be 3.82 (3.95) when $\vec{E}//[001]$ and 2.97 (3.15) $\vec{E}//[010]$ or $\vec{E}//[100]$.

The extinction coefficient is another optical parameter which describes the attenuation of the electromagnetic radiation in a specific medium. Once again, there is a clear similarity between the pattern of $k(\omega)$ and $\varepsilon_2(\omega)$. In the lower energy part, $k(\omega)$ is raised rapidly to get a maximum value at the lower (higher) part of the visible spectrum when $\vec{E}//[001]$ $\vec{E}//[100]$ ($\vec{E}//[010]$).

The reflection coefficient $R(\omega)$ characterizes the part of energy reflected at the interface of the solid. The reflectivity spectra of our Na_2CuPn compounds (Pn = As, P) are shown in **Figures III.8.e** and **III.9.k** . Both compounds show an almost moderate and constant reflectivity in a spread region of the electromagnetic radiation ranging from the zero frequency limit up to the extreme UV region wich vanishes so far.

The frequency dependent absorption coefficients of Na_2CuP and Na_2CuAs are depicted in **Figures III.8.f** and **III.9.l** The obtained results show that both materials are characterized by a wide spread high absorption band in the extreme UV region, giving evidence for a potential optical activity.

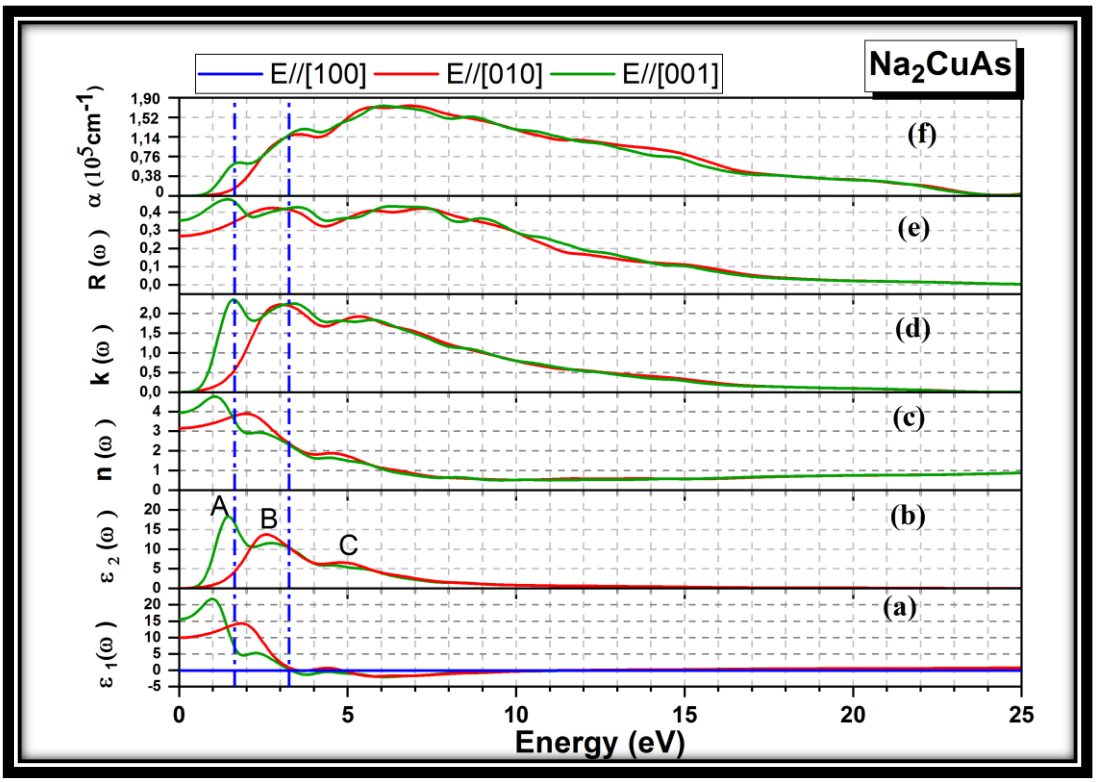

***Figure III.8**: calculated frequency dependent optical parameters for Na_2CuAs*

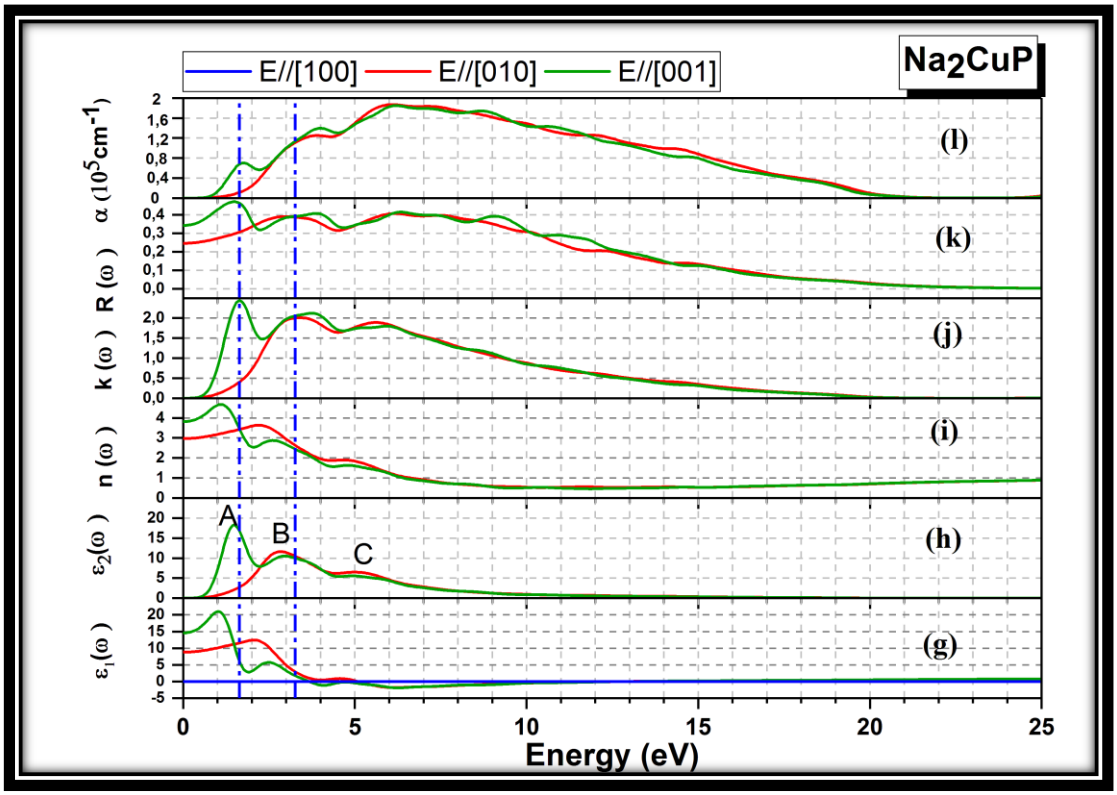

***Figure III.9**: calculated frequency dependent optical parameters for Na_2CuP*

Bibliographical references

1. Segall, M., et al., *First-principles simulation: ideas, illustrations and the CASTEP code.* Journal of Physics: Condensed Matter, 2002. **14**(11): p. 2717.

2. Vanderbilt, D., *Soft self-consistent pseudopotentials in a generalized eigenvalue formalism.* Physical Review B, 1990. **41**(11): p. 7892-7895.

3. Koelling, D.D. and B.N. Harmon, *A technique for relativistic spin-polarised calculations.* Journal of Physics C: Solid State Physics, 1977. **10**(16): p. 3107-3114.

4. Monkhorst, H.J. and J.D. Pack, *Special points for Brillouin-zone integrations.* Physical Review B, 1976. **13**(12): p. 5188-5192.

5. Hellmann, H., *Einfüring in Quantumchemie (Franz Deuticke, Leipzig) 285 Feynman RP 1939 Phys.* Rep, 1937. **56**: p. 340.

6. Feynman, R.P., *Forces in Molecules.* Physical Review, 1939. **56**(4): p. 340-343.

7. Savelsberg, G. and H. Schäfer, *Darstellung und Kristallstruktur von Na2CuP, K2AgAs, K2AgSb und K2AgBi/Preparation and Crystal Structure of Na2CuP, K2AgAs, K2AgSb, and K2AgBi.* Zeitschrift für Naturforschung B, 1977. **32**(7): p. 745-748.

8. Eisenmann, B., G. Savelsberg, and H. Schäfer, *Zur Darstellung und Kristallstruktur von Na2CuAs, K2CuAs und K2CuSb.* Zeitschrift für Naturforschung B, 1976. **31**(10): p. 1344-1346.

9. Anglada, J.M. and J.M. Bofill, *How good is a Broyden–Fletcher–Goldfarb–Shanno-like update Hessian formula to locate transition structures? Specific reformulation of Broyden–Fletcher–Goldfarb–Shanno for optimizing saddle points.* Journal of computational chemistry, 1998. **19**(3): p. 349-362.

10. Broyden, C.G., *The convergence of a class of double-rank minimization algorithms: 2. The new algorithm.* IMA journal of applied mathematics, 1970. **6**(3): p. 222-231.

11. Fletcher, R., *A new approach to variable metric algorithms.* The computer journal, 1970. **13**(3): p. 317-322.

12.Goldfarb, D., *A family of variable-metric methods derived by variational means.* Mathematics of computation, 1970. **24**(109): p. 23-26.

13.Shanno, D.F., *Conditioning of quasi-Newton methods for function minimization.* Mathematics of computation, 1970. **24**(111): p. 647-656.

14. Caro, M.A., S. Schulz, and E.P. O'Reilly, *Comparison of stress and total energy methods for calculation of elastic properties of semiconductors.* Journal of Physics: Condensed Matter, 2012. **25**(2): p. 025803.
15. Mouhat, F. and F.-X. Coudert, *Necessary and sufficient elastic stability conditions in various crystal systems.* Physical Review B, 2014. **90**(22).
16. Born, M., *On the stability of crystal lattices. I.* Mathematical Proceedings of the Cambridge Philosophical Society, 2008. **36**(02).
17. Voigt, W., *Lehrbuch der kristallphysik (mit ausschluss der kristalloptik).* 1946, Leipzig; Berlin; [Ann Arbor, Mich.]: B.G. Teubner [J.W. Edwards].
18. Reuss, A., *Berechnung der fließgrenze von mischkristallen auf grund der plastizitätsbedingung für einkristalle.* ZAMM-Journal of Applied Mathematics and Mechanics/Zeitschrift für Angewandte Mathematik und Mechanik, 1929. **9**(1): p. 49-58.
19. Hill, R., *The elastic behaviour of a crystalline aggregate.* Proceedings of the Physical Society. Section A, 1952. **65**(5): p. 349.
20. Chen, X.-Q., et al., *Modeling hardness of polycrystalline materials and bulk metallic glasses.* Intermetallics, 2011. **19**(9): p. 1275-1281.
21. Pugh, S.F., *XCII. Relations between the elastic moduli and the plastic properties of polycrystalline pure metals.* The London, Edinburgh, and Dublin Philosophical Magazine and Journal of Science, 2009. **45**(367): p. 823-843.
22. Lakes, R., *Foam structures with a negative Poisson's ratio.* Science, 1987. **235**: p. 1038-1041.

General conclusion

General conclusion

Based on the density functional theory (DFT) and the pseudopotential and plane waves approaches as implemented in the CASTEP code, we presented an ab-initio study of the structural, elastic, electronic and optical properties of the orthorhombic polar intermetallic phases Na_2AuPn (Pn = As, P). The exchange-correlation potential is processed in the generalized gradient approximation GGA-PBE. This study is guided by an important goal, which is to explore the physical properties of these two compounds so far unexplored, taking into account three major aspects: the mechanical stability of these materials, their mechanical properties, their electronic structures and their optical properties.

The chosen approach reproduces accurately the equilibrium geometry of these materials. This claims the validity of the methodology and the approximations adopted here. The tensor of the elastic constants fulfils the mechanical Born stability conditions, and consequently the orthorhombic structure of our studied compounds is mechanically stable. The low values of the bulk modulus B, shear modulus G and the Vickers hardness indicate that the studied materials are soft and easily compressible. The calculated B / G ratio show that Na_2CuAs and Na_2CuP are fragile materials. Moreover, these compounds are characterized by low values of the Debye temperature, meaning that they have low thermal conductivities and low heat capacities. The obtained values for the universal anisotropy index give evidence for an anisotropic elastic behavior which comes mainly from anisotropy in shear. We confirmed this result by the study of the directional dependence of the compressibility ad Young's modulus. The energy band structure calculations show that these materials are narrow-gap semiconductors with an indirect band-gap for both materials. Mulliken charges analysis and band populations for both systems give evidence for appreciable covalent interactions between the Cu and P atoms, and between cooper atoms along the zigzag chains and a purely ionic character for the Cu-As bond. A set of frequency dependent optical parameters is calculated for a wide-ranging photon energy and for polarization of the incident electromagnetic radiation parallel to the principal directions [100], [010] and [001]. The obtained results show that both compounds are active in the extreme UV region.

Due to the lack of previous studies (experimental or theoretical) on the physical properties of these materials, our results therefore, can be considered as a guide for future studies. At the end, we hope that our work will allow opening new perspectives in the study of these materials.

ملخص

خصصت هذه الدراسة لمعاينة الخصائص الفيزيائية الغير مدروسة للمركبات القطبية الثلاثية (Na_2CuAs, Na_2CuP). وقد أولينا أهمية قصوى لدراسة خصائصها البنيوية ,المرونية, الإلكترونية والضوئية و ذلك باستخدام برنامج CASTEP الذي يعتمد نظرية دالية الكثافة (DFT) في ظل مبدأ الكمونات المستعارة (pseudopotoniel) و الأمواج المستوية (plan waves) . من بين العديد من التقريبات لحساب طاقة التبادل و الترابط ، استعملنا تقريب التدرج المعمم (GGA-PBE). البنية البلورية للحالة الأساسية في ظل المقاربة النظرية المعتمدة كانت على توافق ممتاز مع النتائج التجريبية. تبين من خلال دراسة الخصائص المرونية أن المركبين Na_2CuAsوNa_2CuP ذوي طبيعة هشة.وغيرمتماثلي المناحي . أظهرت الخصائص الإلكترونية أن هاتين المادتين عبارة عن أشباه موصلات ذات فجوات طاقة صغيرة غير مباشرة. وفي دراسة لطبيعة الروابط بين الذرات تبيّن أنها ذات طبيعة تساهمية بين ذرات النحاس على مدى المحور c في السلسلة المتعرجة و يكمن الفرق بين المركبين في طبيعة الرابطة المتشكلة بين Cu و Pn اذ يسود عليها الطابع التساهمي في Na_2CuP و الطبيعة الأيونية الصرفة في Na_2CuAs . أظهرت دراسة الخصائص الضوئية اين قمنا بحساب دالة العزل و قرينة الانكسار وشدة الامتصاص وبعض الخصائص الأخرى ان هذه المركبات نشطة في مجال الاشعة الفوق بنفسجية القصوى.

كلمات مفتاحية : نظرية دالية الكثافة ,تقريب التدرج المعمم ,الخصائص البنيوية, الخصائص الإلكترونية ,الخصائص المرونية,أشباه الموصلات ,المركبات القطبية الثلاثية.

Abstract

This study is aimed to report on the hitherto unexplored physical properties of the ternary polar intermetallic compounds (Na_2CuAs, Na_2CuP). Particular attention is paid to investigate their structural, elastic, electronic and optical properties. We make use of the GGA-PBE approximation as implemented in the CASTEP code. Based on the plan waves and pseudopotenial approaches of DFT, the obtained results agree well with the available experimental data. This study showed that Na_2CuAs and Na_2CuP were brittle in nature and anisotropic. The predicted electronic properties show that these materials are narrow-gap semiconductors with an indirect band-gap for both materials. Mulliken charges analysis and band populations for both systems give evidence for appreciable covalent interactions between the Cu and P atoms, and between cooper atoms along the zigzag chains and a purely ionic character for the Cu-As bond. A set of frequency dependent optical parameters were calculated including the complex dielectric function, the refractive index and the absorption coefficient. The obtained results show that both compounds are active in the extreme UV region.

Key words: **DFT, GGA, Structural, electronic, elastic properties, semiconductor, polar intermetallic compounds.**

Résumé

Dans Cette étude les propriétés physiques, à ce jour inexplorées des intermétalliques polaires (Na_2CuAs, Na_2CuP) sont étudiées. Un intérêt particulier est accordé à leurs propriétés structurelles, élastiques, électroniques et optiques. Nous avons opté pour une étude théorique de ces composés en utilisant le code CASTEP, qui repose sur la DFT et l'approche du pseudo potentiel et celui des ondes planes. Parmi les nombreuses approximations permettant de calculer l'énergie d'échange et de corrélation, nous avons adopté l'approximation GGA-PBE (GGA). Les résultats obtenus s'accordent parfaitement avec les résultats expérimentaux disponible. L'étude a montré que les deux composées sont fragiles et anisotropes. Les propriétés électroniques montrent que ces matériaux sont des semi-conducteurs à bande interdite étroite et un gap indirect. L'analyse des populations de Mulliken montre que l'interaction entre les atomes Cu et P, et entre les atomes de cuivre le long des chaînes en zigzag est covalente. Tandis qu'elle est d'un caractère purement ionique pour la liaison Cu-As. Un ensemble de paramètres optiques incluant la fonction diélectrique complexe, l'indice de réfraction, et le coefficient d'absorption ont été calculés. Les résultats montrent que ces matériaux sont actifs dans extrême UV.

Mots clés : **DFT, GGA, propriétés structural, élastiques, électroniques, semi-conducteurs, intermétalliques polaires triangulaires.**